

Extending GLUE with Multilevel Methods to Accelerate Statistical Inversion of Hydrological Models

M. G. Rudolph¹, T. Wöhling^{2,3}, T. Wagener⁴, A. Hartmann¹

¹Institute of Groundwater Management, Technische Universität Dresden, Dresden, Germany

²Chair of Hydrology, Institute of Hydrology and Meteorology, Technische Universität Dresden, Dresden, Germany

Germany

³Lincoln Agritech, Lincoln, New Zealand

⁴Institute of Environmental Science and Geography, University of Potsdam, Potsdam, Germany

Key Points:

- Generalized Likelihood Uncertainty Estimation (GLUE) is extended to a setting with multiple levels of model accuracy (MLGLUE)
- MLGLUE reduced the time of inversion for a groundwater flow model by $\approx 45\%$ and $\approx 57\%$ compared to GLUE and standard Markov-chain Monte Carlo
- MLGLUE is especially well-suited for models that discretize independent variables but is shown to be applicable in more general settings

Corresponding author: M. G. Rudolph, max_gustav.rudolph@tu-dresden.de

16 Abstract

17 Inverse problems are ubiquitous in hydrological modelling for parameter estimation,
18 system understanding, sustainable water resources management, and the operation
19 of digital twins. While statistical inversion is especially popular, its sampling-based nature
20 often inhibits the inversion of computationally costly models, which has compromised
21 the use of the Generalized Likelihood Uncertainty Estimation (GLUE) methodology, e.g.,
22 for spatially distributed (partial) differential equation based models. In this study
23 we introduce multilevel GLUE (MLGLUE), which alleviates the computational burden
24 of statistical inversion by utilizing a hierarchy of model resolutions. Inspired by
25 multilevel Monte Carlo, most parameter samples are evaluated on lower levels with
26 computationally cheap low-resolution models and only samples associated with a likelihood
27 above a certain threshold are subsequently passed to higher levels with costly high-resolution
28 models for evaluation. Inferences are made at the level of the highest-resolution model
29 but substantial computational savings are achieved by discarding samples with low likelihood
30 already on levels with low resolution and low computational cost. Two test problems
31 demonstrate the similarity of inferred parameter posteriors and uncertainty estimates
32 of MLGLUE and GLUE as well as increased computational efficiency. Findings are
33 furthermore compared to inversion results from Markov-chain Monte Carlo (MCMC)
34 and from multilevel delayed acceptance MCMC. The computation time of inversion of
35 a groundwater flow model was decreases by $\approx 45\%$ and $\approx 57\%$ when using MLGLUE
36 instead of conventional formulations of GLUE and MCMC, respectively.

37 1 Introduction

38 Inverse problems are ubiquitous in hydrological modelling, emerging in the context
39 of parameter estimation, system understanding, sustainable water resources management,
40 and the operation of digital twins (e.g., Leopoldina, 2022). Inverse problems in this
41 context are often severely ill-posed, resulting in uncertainties associated with computational
42 models (Beven, 1993; Carrera et al., 2005; Beven, 2006; Vrugt et al., 2009; Zhou et al.,
43 2014; Mai, 2023). Considering hydrological system complexity and limited data availability,
44 these uncertainties therefore need to be quantified (Blöschl et al., 2019). While
45 process-based spatially distributed models are often needed to adequately guide decision-
46 making and to sustainably manage water resources, such modelling approaches are
47 computationally costly (Doherty, 2015; Herrera et al., 2022), making uncertainty quantifi-
48 cation (UQ) and statistical inversion especially challenging (Erdal & Cirpka, 2020; Kuffour
49 et al., 2020; White, Hunt, et al., 2020). There is a need to develop computationally
50 efficient approaches to UQ and statistical inversion to overcome the pressing challenges
51 associated with climate change and their impact on water resources.

52 Various approaches to UQ have been developed and applied in that respect; the
53 Bayesian approach to statistical inversion and UQ, however, is especially popular due
54 to the ability to comprehensively treat uncertainties in state variables, parameters, and
55 model output (Montanari, 2007; Vrugt, 2016; Linde et al., 2017; Page et al., 2023). Gen-

56 eralized Likelihood Uncertainty Estimation (GLUE) (Beven & Binley, 1992, 2014; Mirzaei
57 et al., 2015) - as an informal Bayesian approach - and Markov-chain Monte Carlo sam-
58 pling (MCMC) (Gallagher et al., 2009; Vrugt, 2016; Dodwell et al., 2019; Brunetti et al.,
59 2023; Lykkegaard et al., 2023) - as a formal Bayesian approach - are frequently applied
60 in the environmental sciences for statistical inversion. The Bayesian framework consid-
61 ers model parameters to be random variables that are associated with a prior distribu-
62 tion, which is conditioned on system state observations using a likelihood function to form
63 a posterior distribution. The likelihood function may either be defined formally (often
64 requiring knowledge about sources of model error as well as assuming independent and
65 identically distributed errors) or informally (aggregating all aspects of error to a gener-
66 alized fuzzy belief) (Beven & Binley, 1992; Beven & Freer, 2001). Alternatively, likelihood-
67 free methods such as approximate Bayesian computation may be used (Nott et al., 2012;
68 Sadegh & Vrugt, 2013; Beven, 2016; Vrugt & Beven, 2018).

69 Approaches to statistical inversion generally rely on repeatedly running the com-
70 putational model with different parameter values to obtain simulated equivalents of ob-
71 servations. With computationally costly models, this approach quickly becomes intractable
72 and there is a need to develop more efficient sampling approaches for statistical inver-
73 sion. Different approaches have been developed to reduce computational cost of inver-
74 sion, such as using data-driven surrogate or reduced-order models (Doherty & Christensen,
75 2011; Asher et al., 2015; Burrows & Doherty, 2015; Linde et al., 2017; Gosses & Wöhling,
76 2019, 2021; Allgeier, 2022) during inversion, often run instead of the computationally costly
77 high-fidelity model. Reducing model spatial resolution can reduce model complexity and
78 computational cost in general and the effect of horizontal (Wildemeersch et al., 2014)
79 as well as vertical (White, Knowling, & Moore, 2020) discretization in groundwater model
80 performance has been studied before, also in the context of accelerating inversion (von
81 Gunten et al., 2014).

82 Multilevel methods and multilevel Monte Carlo (MLMC) (Heinrich, 2001; Giles,
83 2008; Cliffe et al., 2011; Giles, 2015), with extensions to multilevel MCMC and multi-
84 level delayed acceptance MCMC (MLMCMC and MLDA, respectively) (Dodwell et al.,
85 2019; Lykkegaard et al., 2023), were previously introduced with a similar motivation. In
86 the context of spatially distributed models, multilevel methods utilize multiple levels of
87 spatial domain resolution. Together with the most finely discretized highest level model,
88 also a number of more coarsely discretized lower level models are considered. Most so-
89 lutions to the forward problem are then carried out on lower levels while the highest level
90 model is called far less frequently, harbouring the potential for large savings in overall
91 computation time. Contrary to surrogate- or reduced-order-model-aided approaches to
92 UQ, multilevel methods make no additional simplifying assumptions about the model
93 and the relevant processes are simulated directly on all levels of resolution. Another such
94 contrast is that the coarsely discretized models are not used instead of the high-fidelity
95 model but they are synergetically used together. Linde et al. (2017) summarize first ap-
96 plications of MLMC for the forward propagation of uncertainties in hydrogeology and

97 hydrogeophysics. We note that multilevel methods may be used regarding the discretiza-
 98 tion of any independent variable, such as spatial coordinates or time.

99 Previous applications of multilevel methods focussed on models with different spa-
 100 tial resolutions (Cliffe et al., 2011; Linde et al., 2017; Dodwell et al., 2019; Lykkegaard
 101 et al., 2023), entailing challenges with model parameterization at different resolutions.
 102 Geostatistical approaches are often used to (initially) parameterize spatially distributed
 103 groundwater flow- or other hydrological models, which simultaneously reduces overpa-
 104 rameterization. To this end, utilizing point measurements of parameters or the combi-
 105 nation with other predictor variables, Gaussian process regression is frequently used to
 106 generate conditioned parameter fields on arbitrary spatial resolution (Kitanidis & Vomvoris,
 107 1983; Zimmerman et al., 1998; Zhou et al., 2014; Doherty, 2003). Unconditioned random
 108 fields are also often used, where parameter fields are generated on arbitrary spatial res-
 109 olution (Y. Liu et al., 2019); using uncorrelated and spatially independent random vari-
 110 ables, the Karhunen-Loève expansion is often used to parameterize the random field (Cliffe
 111 et al., 2011; Dodwell et al., 2019; Lykkegaard et al., 2023). The definition of hydrolog-
 112 ical response units or internally homogeneous zones of parameters represents another strat-
 113 egy for parameterization (Kumar et al., 2013; Zhou et al., 2014; Anderson et al., 2015;
 114 White, 2018). To better constrain the parameter space during inversion and to reduce
 115 the aggravating effect of overparameterization, regularization can be employed in com-
 116 bination with different parameterization strategies (Tonkin & Doherty, 2005; Moore &
 117 Doherty, 2006; Pokhrel et al., 2008; Moore et al., 2010). Parameter scaling can be used
 118 to transfer parameter fields from one spatial resolution to another. While there is no gen-
 119 erally valid theory for upscaling (i.e., from fine to coarse grid) (Binley et al., 1989; Samaniego
 120 et al., 2010), various upscaling operators are used in practice (Binley et al., 1989; Samaniego
 121 et al., 2010; Colecchio et al., 2020).

122 While multilevel methods have previously been used to accelerate MCMC algorithms
 123 (Dodwell et al., 2019; Lykkegaard & Dodwell, 2022; Lykkegaard et al., 2023) in a for-
 124 mal Bayesian framework, it has not yet been attempted for GLUE. In this study, we uti-
 125 lize ideas from multilevel Monte Carlo strategies to accelerate statistical inversion of hy-
 126 drological models with the GLUE methodology. After introducing multilevel GLUE (ML-
 127 GLUE), two example inverse problems are considered. We subsequently apply conven-
 128 tional GLUE and MLGLUE as well as MCMC and MLDA to those problems and com-
 129 pare the results.

130 2 The Inverse Problem

131 Consider observations $\tilde{\mathbf{Y}} = [\tilde{y}_1, \dots, \tilde{y}_k]^T \in \mathcal{Y} \subseteq \mathbb{R}^k$ of a real system, made with
 132 measurement error $\boldsymbol{\varepsilon} \in \mathbb{R}^k$. Also consider a model \mathcal{F} that simulates the system response
 133 $\mathbf{Y} = [y_1, \dots, y_k]^T \in \mathcal{Y}$ corresponding to $\tilde{\mathbf{Y}}$. The model output also depends on initial
 134 and boundary conditions \mathcal{C}_i and \mathcal{C}_b , respectively, as well as on model parameters $\boldsymbol{\theta} \in$
 135 $\mathcal{X} \subseteq \mathbb{R}^n$

$$\tilde{\mathbf{Y}} = \mathcal{F}(\boldsymbol{\theta}, \mathcal{C}_i, \mathcal{C}_b) + \boldsymbol{\varepsilon} := \mathcal{F}(\boldsymbol{\theta}) + \boldsymbol{\varepsilon} \quad (1)$$

136 $\mathcal{F} : \mathcal{C}_i, \mathcal{C}_b \rightarrow \mathbf{Y} \in \mathcal{Y}$ is closed by the parameter vector $\boldsymbol{\theta}$ (Kavetski et al., 2006; Vrugt
 137 et al., 2009), which is considered a random vector with an associated prior distribution
 138 $p_p(\boldsymbol{\theta})$. Solving the inverse problem in a Bayesian statistical framework means to obtain
 139 the posterior distribution of the parameters $p(\boldsymbol{\theta}|\tilde{\mathbf{Y}})$ via Bayes' theorem

$$p(\boldsymbol{\theta}|\tilde{\mathbf{Y}}) = \frac{p_p(\boldsymbol{\theta})p(\tilde{\mathbf{Y}}|\boldsymbol{\theta})}{p(\tilde{\mathbf{Y}})} \propto p_p(\boldsymbol{\theta})p(\tilde{\mathbf{Y}}|\boldsymbol{\theta}) \quad (2)$$

140 where $p_p(\boldsymbol{\theta})$ is the prior parameter distribution, $p(\tilde{\mathbf{Y}}|\boldsymbol{\theta})$ is the likelihood function, and
 141 $p(\tilde{\mathbf{Y}})$ is the evidence.

142 Assuming that model errors $r_i = y_i - \tilde{y}_i$ are mutually independent and identi-
 143 cally distributed (i.i.d.) and follow a Gaussian distribution with constant variance σ_r^2 ,
 144 the log-likelihood takes the form

$$\mathcal{L}(\boldsymbol{\theta}|\tilde{\mathbf{Y}}) = -\frac{k}{2} \ln(2\pi) - \frac{k}{2} \ln(\sigma_r^2) - \frac{1}{2} \sigma_r^2 \cdot \sum_{i=1}^k (y_i - \tilde{y}_i)^2 \quad (3)$$

145 The assumptions of i.i.d. model errors, however, usually does not hold as hydrological
 146 model errors often exhibit strong autocorrelation and heteroscedasticity (see, e.g., Beven
 147 (2006) for a discussion). Beven and Freer (2001) and Vrugt et al. (2009) give alterna-
 148 tive likelihood formulations that deal with those issues, often at the cost of additional
 149 hyperparameters.

150 2.1 Multilevel Methods

151 We will discuss the notion of multilevel methods from the perspective of multilevel
 152 Monte Carlo (MLMC), which is a method to efficiently compute the expectation of a quan-
 153 tity of interest that depends on (model) parameters (Heinrich, 2001; Giles, 2008; Cliffe
 154 et al., 2011; Giles, 2015). While MLMC is used for the forward propagation of uncer-
 155 tainty instead of inversion, it builds on a simple intuition that illustrates the idea behind
 156 MLGLUE.

157 As an example, consider the situation where we are given a parameter (posterior)
 158 distribution $p(\boldsymbol{\theta})$ and want to compute the expected value of the model output $\mathbf{Y} = \mathcal{F}(\boldsymbol{\theta})$
 159 with respect to $p(\boldsymbol{\theta})$, which is a problem of propagating parameter uncertainty through
 160 the model. For simplicity and without loss of generality consider $\mathbf{Y} \in \mathbb{R}$ for the remain-
 161 der of this section. Instead of one single model for the system, assume that there is a hi-
 162 erarchy of models (approximations) $\{\mathcal{F}_\ell\}_{\ell=0}^\infty$ such that $\tilde{\mathbf{Y}} = \lim_{\ell \rightarrow \infty} \mathcal{F}_\ell$, where ℓ is the
 163 level index. We assume that the computational cost for evaluating \mathcal{F}_ℓ increases while the
 164 approximation error decreases as $\ell \rightarrow L$. In the context of PDE-based models, ℓ may
 165 be related to the grid size or time step length of the model, i.e., a larger ℓ corresponds
 166 to a structurally more accurate model. To estimate the expectation of \mathbf{Y} efficiently, MLMC
 167 avoids the direct estimation of $\mathbb{E}[\mathcal{F}_L]$ on the highest level $\ell = L$. Instead, the correc-
 168 tion of the estimation with respect to the next lower level is computed, based on the lin-
 169 earity of expectation:

$$\mathbb{E}[\mathcal{F}_L] = \mathbb{E}[\mathcal{F}_0] + \sum_{\ell=1}^L \mathbb{E}[\mathcal{F}_\ell - \mathcal{F}_{\ell-1}] \quad (4)$$

170 This approach generally results in substantial computational savings and different
 171 multilevel estimators for $\mathbb{E}[\mathcal{F}_L]$ exist (Giles, 2008; Cliffe et al., 2011; Giles, 2015; Dod-
 172 well et al., 2019; Lykkegaard et al., 2023). The original MLMC algorithm of Giles (2008)
 173 (as well as subsequently applied algorithms) takes a bottom-up approach, i.e., sampling
 174 is started on $\ell = 0$ and ℓ is only incremented if the algorithm has not yet converged on
 175 level ℓ . There, efficiency and variance reduction regarding the expectation of \mathbf{Y} may be
 176 optimized by choosing an optimal refinement (e.g., the decrease of cell or time step size
 177 when going from ℓ to $\ell + 1$).

178 In the context of MLMC, the behaviour of the variances $\mathbb{V}[\mathcal{F}_\ell]$ and $\mathbb{V}[\mathcal{F}_\ell - \mathcal{F}_{\ell-1}]$
 179 and expectations $\mathbb{E}[\mathcal{F}_\ell]$ and $\mathbb{E}[\mathcal{F}_\ell - \mathcal{F}_{\ell-1}]$ as $\ell \rightarrow L$ gives an indication of the overall
 180 quality and efficiency of the hierarchy $\{\mathcal{F}_\ell\}_{\ell=0}^L$ (Cliffe et al., 2011). $\mathbb{V}[\mathcal{F}_\ell]$ and $\mathbb{E}[\mathcal{F}_\ell]$ should
 181 be approximately constant as $\ell \rightarrow L$, ensuring that \mathcal{F}_ℓ is a good enough approxima-
 182 tion even on the coarsest level $\ell = 0$. Furthermore, $\mathbb{V}[\mathcal{F}_\ell - \mathcal{F}_{\ell-1}]$ and $\mathbb{E}[\mathcal{F}_\ell - \mathcal{F}_{\ell-1}]$
 183 should decay rapidly as $\ell \rightarrow L$, ensuring that the approximation error decreases with
 184 increasing level. $\mathbb{V}[\mathcal{F}_\ell - \mathcal{F}_{\ell-1}]$ may be expanded as

$$\mathbb{V}[\mathcal{F}_\ell - \mathcal{F}_{\ell-1}] = \mathbb{V}[\mathcal{F}_\ell] + \mathbb{V}[\mathcal{F}_{\ell-1}] - 2 \cdot \text{Cov}(\mathcal{F}_\ell, \mathcal{F}_{\ell-1}), \quad (5)$$

185 showing that it should be given that $2 \cdot \text{Cov}(\mathcal{F}_\ell, \mathcal{F}_{\ell-1}) > \mathbb{V}[\mathcal{F}_{\ell-1}]$, which requires \mathcal{F}_ℓ
 186 and $\mathcal{F}_{\ell-1}$ to be sufficiently correlated.

187 While those relations between levels are not formally required to hold for inversion,
 188 they ensure that the multilevel estimator for the expectation of \mathbf{Y} has reduced variance
 189 and is computationally more efficient compared to a single-level estimator (Cliffe et al.,
 190 2011; Lykkegaard et al., 2023). While a deviation of the previously described optimal
 191 relations between levels does not necessarily indicate a poorly performing model hier-
 192 archy, without such a deviation the hierarchy may be said to be well behaved.

193 During multilevel inversion, no explicit approach exists yet to pre-define (or opti-
 194 mize) the number of levels or the refinement (or coarsening, respectively). Dodwell et
 195 al. (2019); Lykkegaard et al. (2023) arbitrarily pre-define the coarsening as well as the
 196 number of levels considered but give some analysis of the effect regarding the number
 197 of levels. In similar examples to our subsequently considered benchmark example of ground-
 198 water flow, Cliffe et al. (2011) consider 5 levels, Dodwell et al. (2019) consider up to 5
 199 levels, Lykkegaard and Dodwell (2022) consider 2 levels, and Lykkegaard et al. (2023)
 200 consider 3 levels.

201 2.2 Multilevel Markov-chain Monte Carlo

202 The multilevel delayed acceptance (MLDA) MCMC algorithm was developed by
 203 Lykkegaard et al. (2023) on the basis of the delayed acceptance algorithm coupled with
 204 the randomized-length-subchain surrogate transition (Christen & Fox, 2005; J. S. Liu,
 205 2008). The main functionality of MLDA is shown in Fig. 1 for a case with two levels.
 206 We use the Python implementation of MLDA by Lykkegaard (2022) with fixed-length
 207 subchains and the option of running a number of n_{chains} chains in parallel. In the re-

208 mainder we also assume that the parameter vectors $\{\boldsymbol{\theta}_\ell\}_{\ell=0}^L$ are comprised of the same
 209 model parameters, i.e., we do not consider level-dependent or different coarse and fine
 210 (or nested) model parameter vectors.

211 While other MCMC algorithms sample from a single (posterior) distribution as given
 212 in Eq. 2, MLDA considers a hierarchy of distributions $p_0(\cdot), \dots, p_\ell(\cdot), \dots, p_L(\cdot)$ that are
 213 computationally cheap approximations of the target density $p(\cdot)$, where each $p_\ell(\cdot)$ may
 214 be defined according to Eq. 2 corresponding to each model in $\{\mathcal{F}_\ell\}_{\ell=0}^L$. The MLDA al-
 215 gorithm then gets called on the highest level density $p_L(\cdot)$. By recursively calling the MLDA
 216 algorithm on level $\ell - 1$, subchains with length J_ℓ are generated on levels $1 \leq \ell \leq L$
 217 until level $\ell = 0$ is reached. We note that different subchain lengths may be used on
 218 different levels but the analysis here is restricted to the same $J_\ell = J$ on all levels. On
 219 the lowest level $\ell = 0$, a conventional MCMC sampler is invoked. The final state of a
 220 subchain on level $\ell - 1$, $\boldsymbol{\theta}_{\ell-1}^{J_\ell}$, is finally passed as a proposal to the higher-level chain
 221 on level ℓ . Subsequently, only samples from the highest level are considered for inference.
 222 A conventional single-level MCMC sampler may be obtained with using MLDA if only
 223 the highest-level model is considered. We note that for MLDA the relation between dif-
 224 ferent levels is not formally required to show decaying variance and mean as described
 225 in section 2.1.

226 As with any MCMC algorithm, MLDA posterior uncertainty estimates for (highest-
 227 level) model outputs may be computed as confidence intervals from simulations made
 228 with posterior samples, which are obtained during sampling. MCMC (and MLDA) sam-
 229 ples are naturally correlated and may show dependence on initial samples, requiring that
 230 an initial number of samples are burned and that that samples are thinned (e.g., every
 231 other sample may be omitted to reduce autocorrelation) (e.g., Vrugt, 2016; Lykkegaard
 232 et al., 2023). To assess convergence of the Markov-chains, the Gelman-Rubin statistic
 233 \widehat{R} is frequently used for multi-chain samplers (Gelman & Rubin, 1992). A value of $\widehat{R} \leq$
 234 1.2 is often deemed sufficient to ensure convergence (e.g., Vrugt, 2016).

235 **2.3 Multilevel Generalized Likelihood Uncertainty Estimation**

236 The Generalized Likelihood Uncertainty Estimation (GLUE) methodology rejects
 237 the formal (Bayesian) statistical basis of inference and instead seeks to identify a set of
 238 system representations (combinations of model inputs, model structures, model param-
 239 eters, model errors) that are sufficiently consistent with the observations of that system
 240 (Beven & Freer, 2001; Vrugt et al., 2009; Beven & Binley, 2014; Mirzaei et al., 2015). In
 241 the GLUE methodology the models used for inference are not considered to be true, con-
 242 trary to the case of formal Bayesian inversion.

243 The likelihood function in GLUE aggregates all aspects of error and consistency
 244 as a generalized fuzzy belief. It serves as a decision threshold to separate behavioural
 245 (i.e., good agreement between \mathbf{Y} and $\widetilde{\mathbf{Y}}$) and non-behavioural (i.e., poor agreement be-
 246 tween \mathbf{Y} and $\widetilde{\mathbf{Y}}$) simulations. Beven and Binley (1992) and (Beven & Freer, 2001) in-
 247 troduced a number of different functions for this purpose and the following likelihood

248 is frequently used (Vrugt et al., 2009):

$$\tilde{\mathcal{L}}(\boldsymbol{\theta}|\tilde{\mathbf{Y}}) := (\sigma_r^2)^{-T} = \left(\frac{\sum_{i=1}^k (y_i - \tilde{y}_i)^2}{k-2} \right)^{-T} \quad (6)$$

249 Parameter and model output uncertainty is estimated in GLUE by running the model
 250 with N parameter samples randomly drawn from the prior distribution $\{\boldsymbol{\theta}^{(j)}\}_{j=1}^N$ and
 251 evaluating the likelihood function for each sample. The likelihood threshold may either
 252 be defined a-priori (as a certain value above which a model realization is considered be-
 253 havioural) or may be defined as a percentage based on the set of all likelihood correspond-
 254 ing to the evaluated parameter samples (by setting the threshold to, e.g., the top 10%
 255 of the likelihood values) (Beven & Binley, 1992; Beven & Freer, 2001; Vrugt et al., 2009).
 256 Using only behavioural solutions, (cumulative) probability distributions of model out-
 257 puts are generated, from which uncertainty estimates are finally computed. Behavioural
 258 parameter samples are used to estimate the posterior distribution of model parameters.

259 MLGLUE is generally similar to MLDA (or MLMCMC) as shown in Fig. 1. As with
 260 MLDA, a parameter sample $\boldsymbol{\theta}^{(j)}$ is only finally accepted if it is accepted on the highest
 261 level. While MLDA makes use of an acceptance probability on all levels (as it is typi-
 262 cal in MCMC algorithms), MLGLUE uses a level-dependent likelihood threshold on all
 263 levels to distinguish between samples being accepted (i.e., behavioural solutions) and sam-
 264 ples being discarded (i.e., non-behavioural solutions).

265 MLGLUE requires that likelihood thresholds are available for every level prior to
 266 sampling. While pre-defined likelihood thresholds can optionally be used, MLGLUE im-
 267 plements the estimation of the likelihood thresholds via Monte Carlo sampling, where
 268 an identical set of parameter samples is evaluated on each level. We refer to that as *tun-*
 269 *ing* and the number of tuning samples in that set, N_t , should be substantially smaller
 270 than the overall number of samples being evaluated with MLGLUE, $N_t \ll N$. Calcula-
 271 ting corresponding likelihood values for each of those tuning samples then results in
 272 an individual set of likelihood values for each level. We denote the set of likelihood sam-
 273 ples on a single level by $\{\tilde{\mathcal{L}}^{(i,\ell)}\}_{i=1}^{N_t}$ and the combined set for all levels by $\{\{\tilde{\mathcal{L}}^{(i,\ell)}\}_{i=1}^{N_t}\}_{\ell=0}^L$.
 274 From those sets the likelihood threshold is calculated for each level as a pre-defined per-
 275 centage; we denote the set of likelihood thresholds on each level by $\{\tilde{\mathcal{L}}_{T,\ell}\}_{\ell=0}^L$.

276 From the set of likelihood values on each level, $\{\{\tilde{\mathcal{L}}^{(i,\ell)}\}_{i=1}^{N_t}\}_{\ell=0}^L$, sample estimates
 277 of $\mathbb{V}[\tilde{\mathcal{L}}_\ell]$, $\mathbb{E}[\tilde{\mathcal{L}}_\ell]$, $\mathbb{V}[\tilde{\mathcal{L}}_\ell - \tilde{\mathcal{L}}_{\ell-1}]$, and $\mathbb{E}[\tilde{\mathcal{L}}_\ell - \tilde{\mathcal{L}}_{\ell-1}]$ for $\ell = 0, \dots, L$ are computed to ana-
 278 lyze the relation between levels regarding the likelihood.

279 Afterwards, *sampling* is started and parameter samples $\boldsymbol{\theta}^{(j)}$ are initially evaluated
 280 with the model on level $\ell = 0$. If the corresponding likelihood is greater or equal to the
 281 level-dependent threshold, the sample is passed to the next higher level and is evaluated
 282 again. This process is repeated until the highest level is reached and the sample is finally
 283 considered behavioural or non-behavioural. If the likelihood is smaller than the level-
 284 dependent threshold on any level, the sample is immediately regarded as non-behavioural
 285 and the next sample is considered. Therefore, samples with low likelihood are disregarded

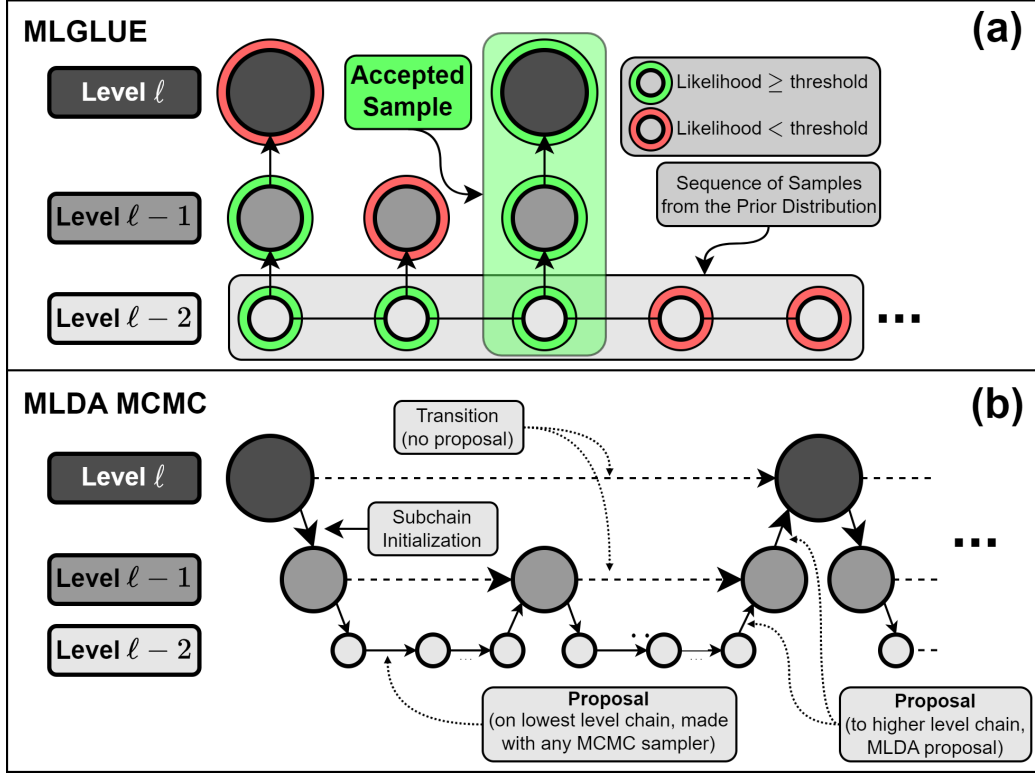


Figure 1. Schematic representation of multilevel sampling strategies for the case of three levels; (a) MLGLUE approach, green rings indicate a likelihood that is above the level-dependent threshold, red rings indicate the contrary; (b) Multilevel Delayed Acceptance MCMC; circles represent the state or current parameter sample

286 already on lower levels, leading to substantial computational savings. In the support-
 287 ing information, the reasoning for using level-dependent likelihood thresholds as well as
 288 the structure of the algorithm is clarified in more detail.

289 The MLGLUE algorithm is shown in Fig. 2 and involves the following steps dur-
 290 ing sampling (tuning is excluded here):

- 291 1. Draw a sample Θ_0 of N points from the (typically uniform) prior distribution $p_p(\theta)$
 292 and set $j = 0$
- 293 2. Set $\ell = 0$ and
 - 294 (a) Compute the likelihood $\tilde{\mathcal{L}}^{(j,\ell)} = \tilde{\mathcal{L}}(\theta^{(j)}|\tilde{\mathbf{Y}})$ with sample $\theta^{(j)}$ from Θ_0 and with
 295 the model on level ℓ
 - 296 i. if $\ell = L$ and $\tilde{\mathcal{L}}^{(j,\ell)} \geq \tilde{\mathcal{L}}_{T,\ell}$, store $\theta^{(j)}$ in matrix \mathbf{B} , increment $j \leftarrow j + 1$,
 297 and go back to step 2
 - 298 ii. if $\tilde{\mathcal{L}}^{(j,\ell)} \geq \tilde{\mathcal{L}}_{T,\ell}$, increment $\ell \leftarrow \ell + 1$ and go back to step 2a
 - 299 iii. if $\tilde{\mathcal{L}}^{(j,\ell)} < \tilde{\mathcal{L}}_{T,\ell}$, increment $j \leftarrow j + 1$ and go back to step 2

- 300 iv. if $j = N$, break the iteration and go to step 3
- 301 3. For each $i = 1, \dots, N_b$ in \mathbf{B} , normalize the corresponding likelihood via $\tilde{\mathcal{L}}'(\mathbf{B}^{(i)}|\tilde{\mathbf{Y}}) =$
- 302 $\tilde{\mathcal{L}}(\mathbf{B}^{(i)}|\tilde{\mathbf{Y}}) / \sum_{i'=1}^{N_b} \tilde{\mathcal{L}}(\mathbf{B}^{(i')}|\tilde{\mathbf{Y}})$
- 303 4. For each $\mathbf{Y}^i, i = 1, \dots, N_b$ in \mathbf{B} , assign the corresponding probability $\tilde{\mathcal{L}}'(\mathbf{B}^{(i)}|\tilde{\mathbf{Y}})$
- 304 5. Sort the $\mathbf{Y}^i, i = 1, \dots, N_b$ increasingly according to their probability and create
- 305 uncertainty intervals from the obtained distribution

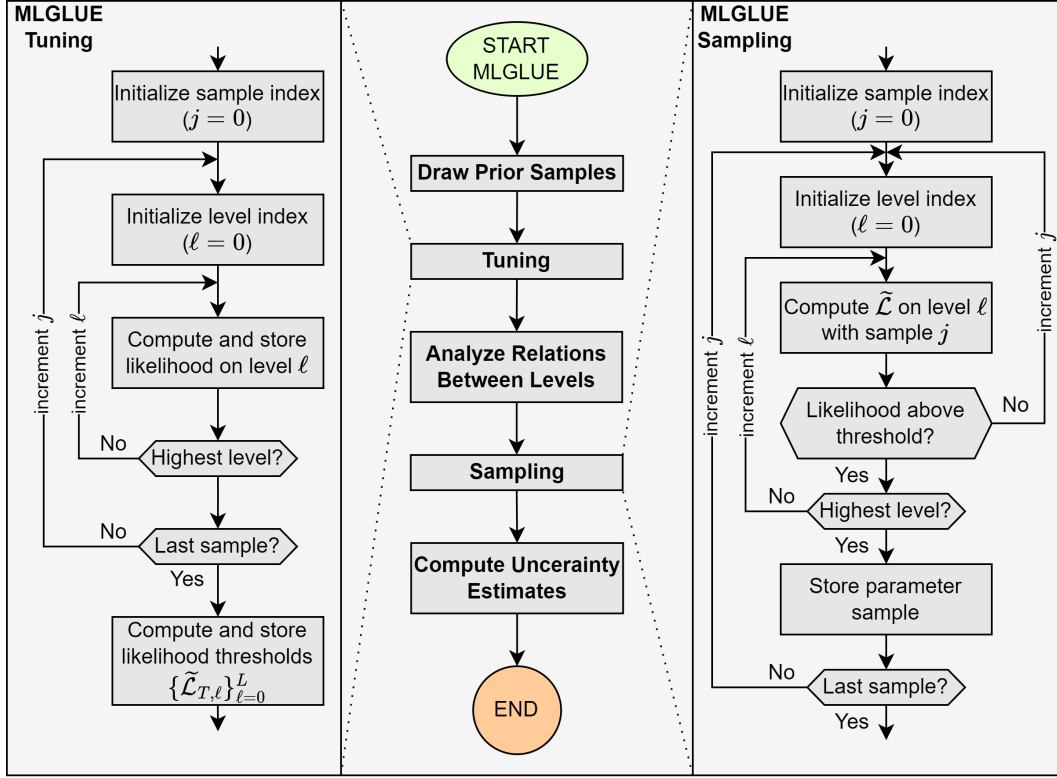


Figure 2. Schematic representation of the multilevel Generalized Likelihood Uncertainty Estimation algorithm; tuning refers to the (optional) Monte Carlo estimation of likelihood thresholds, sampling refers to the repeated evaluation of parameter samples (see the description of algorithm steps)

306 2.4 Convergence Analysis

307 Although the Gelman-Rubin statistic (see section 2.2) is widely used to assess con-
 308 vergence of MCMC chains, the statistic is restricted to multi-chain methods. Because
 309 MLGLUE and GLUE do not operate with multiple chains, we introduce an alternative
 310 methodology to assess convergence.

311 Let \mathbf{B} be the $N \times n$ matrix of samples, where an individual row or column is in-
 312 dexed as $\mathbf{B}_{i,*}$ or $\mathbf{B}_{*,j}$, respectively. The normalized relative deviation \mathcal{D} of a sub-sample

313 of \mathbf{B} , having length i , from the global mean of the corresponding j -th parameter in \mathbf{B}
 314 is then computed as

$$\mathcal{D}_{i,j} = \frac{\frac{1}{i} \sum_{k=1}^i \mathbf{B}_{k,j}}{\frac{1}{N} \sum_{k=1}^N \mathbf{B}_{k,j}} - 1 \quad (7)$$

315 Assessing convergence for all possible i results in a sequence of relative deviations
 316 $\{\mathcal{D}_{i,j}\}_{i=1}^N$ for a parameter j . Bootstrap replicates of $\mathcal{D}_{i,j}$ for each i are then computed,
 317 resulting in average normalized relative deviations from the global mean $\widehat{\mathcal{D}}_{i,j}$. Conver-
 318 gence is assumed when $\widehat{\mathcal{D}}_{i,j}$ continuously stays within a pre-defined tolerance range (e.g.,
 319 ± 0.05). Analyzing after which fraction of N $\widehat{\mathcal{D}}_{i,j}$ continuously stays within a tolerance
 320 range (e.g., ± 0.05) furthermore enables the assessment of convergence behaviour.

321 2.5 Test Problems

322 The test problems discussed in sections 2.5.1 and 2.5.2 are used to show the dif-
 323 ferences between the methods of statistical inference (MLGLUE, GLUE, MLDA, MCMC)
 324 regarding obtained posterior distributions, uncertainty estimates for model output, and
 325 computational efficiency. An identical number of prior parameter samples is used for all
 326 methods to ensure comparability. For GLUE and MLGLUE, an informal (Eq. 6) as well
 327 as a formal (Eq. 3) likelihood function are used for each problem. MCMC and MLDA
 328 are used with a formal likelihood function (Eq. 3). Gaussian (iid) random noise is added
 329 to each set of observations, making the assumptions for defining Eq. 3 valid.

330 The same number of CPUs as well as the same framework for parallelization are
 331 used for all methods. For reasons of reproducibility, seeds are used for pseudo-random
 332 number generation, which is used in multiple places (e.g., drawing samples from a dis-
 333 tribution); the same seeds are used for all methods of inference in the example under study.

334 All methods of inference are implemented in the `Python` programming language.
 335 The `tinyDA v0.9.8` (Lykkegaard, 2022) package is used for MLDA and MCMC sam-
 336 pling with a DREAM(Z)-sampler, which is similar to the DREAM(ZS)-sampler (Vrugt,
 337 2016; Lykkegaard, 2022), using `Ray v2.2.0` (Team, 2022) for parallelization. `ArviZ v0.12.1`
 338 (Kumar et al., 2019) is used for the analysis of MLDA and MCMC results (convergence,
 339 effective sample size); in `tinyDA`, the initial sample is returned additionally to the N .
 340 MLGLUE is implemented as a `Python` package and also enabled for parallel computing
 341 with `Ray v2.2.0` (Team, 2022).

342 2.5.1 Linear Regression

343 The first case study is a simple linear equation in one dimension:

$$f(\boldsymbol{\theta}) = \boldsymbol{\theta}_1 x + \boldsymbol{\theta}_2, \quad x \in [0, 1] \quad (8)$$

$$\tilde{\mathbf{Y}} = f(\boldsymbol{\theta}) + \mathcal{N}(\mu = 0, \sigma = 0.8) \quad (9)$$

344 where θ_1 represents the slope and θ_2 represents the intercept; $\boldsymbol{\theta} = [\theta_1, \theta_2]^T$. A total
 345 of $n = 500$ samples are obtained, forming $\tilde{\mathbf{Y}}$, by calculating $\mathcal{F}(\boldsymbol{\theta})$ for 500 linearly
 346 spaced points $x \in [0, 1]$ with $\theta_1 = 2$ and $\theta_2 = 1$. The true model as well as noisy ob-
 347 servations are shown in Fig. 3.

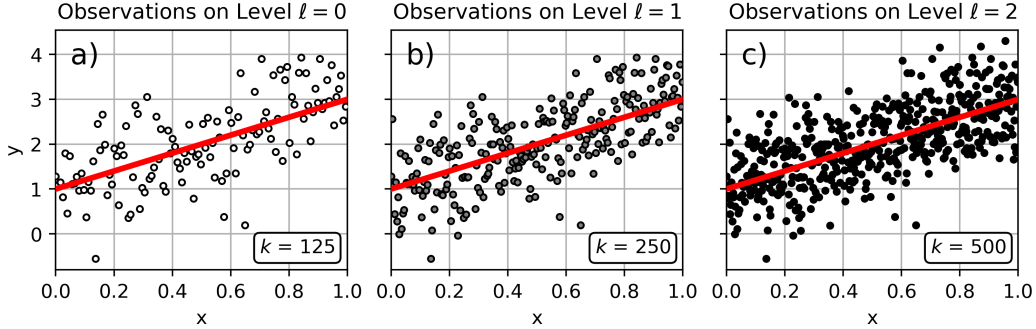


Figure 3. True model (red line) as well as noisy observations on levels $\ell = 0$ (a), $\ell = 1$ (b), and $\ell = 2$ (c) for the regression example

348 Eq. 8 does not need to be discretized as it is a closed-form expression for the sys-
 349 tem response. Similar to the linear regression example from Lykkegaard (2022), the dif-
 350 ferent levels are obtained by considering all observations for the highest level and sub-
 351 sequently removing observations to represent lower levels. We chose the total number
 352 of levels to be 3, i.e., $\ell = 0, 1, 2$, where all 500 observations are considered on level $\ell =$
 353 2, every second observation is considered on level $\ell = 1$, and every fourth observation
 354 is considered on level $\ell = 0$. The different sets of observations are represented in Fig.
 355 3.

356 The prior distribution $p_0(\boldsymbol{\theta})$ is chosen to be a uniform distribution with lower bounds
 357 $\theta_{1,l} = -4$ and $\theta_{2,l} = -2$ and upper bounds $\theta_{1,u} = 4$ and $\theta_{2,u} = 2$. A total number
 358 of $N_t + N = 2,000 + 98,000 = 100,000$ samples are drawn from $p_p(\boldsymbol{\theta})$ with each in-
 359 ference method, where $N_t = 2,000$ samples are used to estimate the level-dependent
 360 likelihood thresholds (see section 2.3) and to analyze the relations between the levels (see
 361 section 2.1) in MLGLUE. A constant variance equal to the constant additive Gaussian
 362 noise variance ($\sigma^2 = 0.8$) is used for the Gaussian likelihood (see Eq. 3); for informal
 363 likelihoods (see Eq. 6) $T = 1$ is used. The likelihood thresholds are estimated to cor-
 364 respond to the best 0.2% of simulations. For MLDA, the sub-sampling rate is set to 5.
 365 All methods are run on 5 CPUs.

366 We note that both likelihood functions used are dependent on the number of ob-
 367 servations considered. With the sum of squared residuals, data variance, and error vari-
 368 ance held constant, the likelihood in Eq. 6 will increase while the likelihood in Eq. 3 will
 369 decrease with an increasing number of observations. Because a different number of ob-
 370 servations is used on different levels in the present problem, this effect weakens the ex-

371 planatory power of the relations between levels (see section 2.1) shown in Fig. 5 (and
 372 in Fig. S1 in the supporting information). This is due to the fact that those opposing
 373 dependencies on the number of observations greatly superimpose the effects of the sum
 374 of squared residuals on the likelihood when going from ℓ to $\ell + 1$.

375 **2.5.2 Groundwater Flow**

376 The second example considers steady-state two-dimensional groundwater flow in
 377 an aquifer with inhomogeneous horizontal hydraulic conductivity, Dirichlet-type (fixed
 378 potentials), Neumann-type (no-flow conditions, recharge), Robin-type (river), and nodal
 379 sink type (wells) boundary conditions:

$$\frac{\partial}{\partial x} \left(K_{xx} \frac{\partial h}{\partial x} \right) + \frac{\partial}{\partial y} \left(K_{yy} \frac{\partial h}{\partial y} \right) + R = 0 \quad (10)$$

$$h = h_c \quad \forall y \in \partial\Omega, x = 0 \text{ m} \quad (11)$$

$$\frac{\partial h}{\partial y} = 0 \quad \forall x \in \partial\Omega, y \in \{0 \text{ m}, 5,000 \text{ m}\} \quad (12)$$

$$\frac{\partial h}{\partial x} = 0 \quad \forall y \in \partial\Omega, x = 10,000 \text{ m} \quad (13)$$

$$f_{riv} = c_{riv} \Delta h \quad \forall 0 \text{ m} \leq x \leq 10,000 \text{ m}, y = 1,000 \text{ m} \quad (14)$$

380 where K [LT^{-1}] is the hydraulic conductivity field, h [L] is the hydraulic head
 381 field, R [LT^{-1}] is the recharge flux, f_{riv} [LT^{-1}] is river inflow, and c_{riv} [T^{-1}] is riverbed
 382 conductance. The model is set up with the finite-differences code `MODFLOW-NWT` and the
 383 reader is referred to Harbaugh (2005) and Niswonger et al. (2011) for a detailed descrip-
 384 tion of the model and boundary condition implementations.

385 The reference model is discretized as a regular structured grid with a cell-size of
 386 $25 \text{ m} \times 25 \text{ m}$, having 200 rows and 400 columns. The aquifer bottom is horizontal at
 387 10.0 m above the reference datum; the aquifer top represents a tilted plane falling lin-
 388 early from 50.0 m on the left side of the domain to 40 m above the reference datum
 389 on the right side of the domain. A river crosses the domain along a single row, having
 390 a constant water level at 1.0 m below the aquifer top and a river bottom at 4.0 m be-
 391 low the aquifer top. 5 wells are placed in the model domain with a total extraction rate
 392 of 700 md^{-1} . Spatially uniform recharge is applied with a rate of $2 \cdot 10^{-5} \text{ md}^{-1}$. A
 393 constant head of 45.0 m above the reference datum is assigned to the leftmost column
 394 of cells. 12 observation points as well as 1 prediction point are placed in the domain.

395 The hydraulic conductivity in every cell is obtained in the reference model using
 396 a regular grid of pilot points (e.g., Doherty, 2003), linearly spaced (5 along columns, 10
 397 along rows) starting on the domain boundaries. Reference values of pilot point hydraulic
 398 conductivities are obtained by sampling from a log-normal distribution with $\mu = 0.3$
 399 and $\sigma = 0.7$. Gaussian process regression (GPR), as implemented in `scikit-learn v1.2.0`
 400 (Pedregosa et al., 2011), is used to interpolate hydraulic conductivities at cell centers of
 401 the reference model with a radial basis function kernel with a fixed length scale of 600 m .

402 The model domain and its main characteristics are shown in Fig. 4 for the models on
 403 levels $\ell = 0$ and $\ell = 3$.

404 The reference model is also the highest-level model. Besides this model, three lower-
 405 level models are considered, resulting in $\ell = 0, 1, 2, 3$. Lower-level models are obtained
 406 via grid coarsening, where cell sizes are doubled going from ℓ to $\ell - 1$. Lower-level hy-
 407 draulic conductivity values at each cell are obtained by using the geometric mean of cor-
 408 responding higher-level cells.

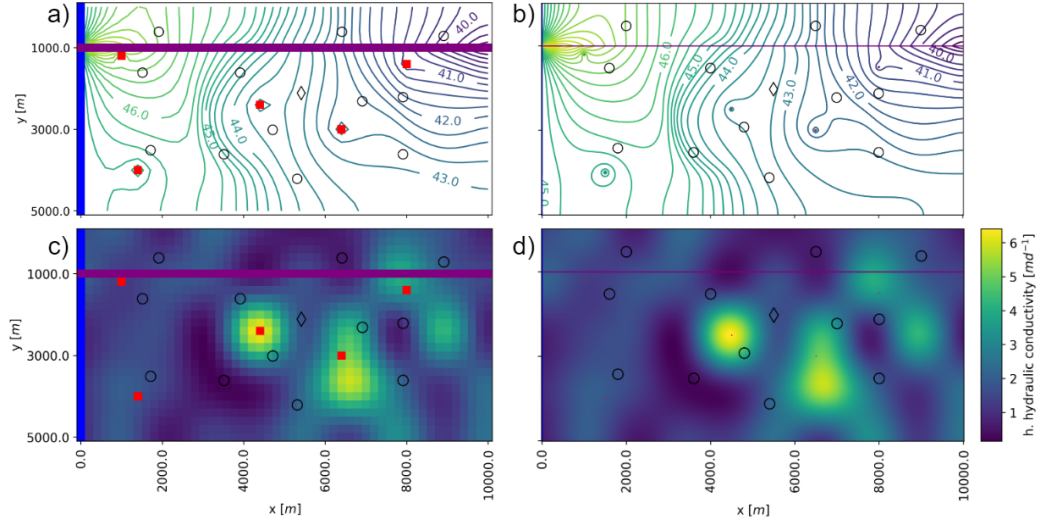


Figure 4. Groundwater flow model domain; head contours obtained with true parameters on level $\ell = 0$ (a) and on level $\ell = 3$ (b); horizontal hydraulic conductivity field on level $\ell = 0$ (c) and on level $\ell = 3$ (d); specific characteristics are: constant head cells (blue), river cells (purple), wells (red), observation points (circles), prediction point (diamond)

409 Besides the 50 pilot point parameters, the GPR length scale is considered a model
 410 parameter as well; $\boldsymbol{\theta} = [\theta_{1,PP}, \dots, \theta_{50,PP}, \theta_{51,GPR}]^T$. We denote the parameter-to-observable
 411 map (i.e., Eqs. 10 to 14) by $\mathcal{M}(\boldsymbol{\theta})$. Adding Gaussian random noise to the observations
 412 then leads to $\tilde{\mathbf{Y}} = \mathcal{M}(\boldsymbol{\theta}) + \mathcal{N}(\mu = 0, \sigma = 1)$.

413 As a prior distribution $p_p(\boldsymbol{\theta})$, a uniform distribution is chosen with lower bounds
 414 $\boldsymbol{\theta}_l = [1 \cdot 10^{-2}, \dots, 1 \cdot 10^{-2}, 5 \cdot 10^2]$ and upper bounds $\boldsymbol{\theta}_u = [1 \cdot 10^1, \dots, 1 \cdot 10^1, 1 \cdot 10^3]$.
 415 A total number of $N_t + N = 2,000 + 98,000 = 100,000$ samples are drawn from $p_0(\boldsymbol{\theta})$
 416 with each inference method, where $N_t = 2,000$ samples are used to estimate the level-
 417 dependent likelihood thresholds (see section 2.3) and to analyze the relations between
 418 the levels (see section 2.1) in MLGLUE. A constant variance equal to the constant ad-
 419 ditive Gaussian noise variance ($\sigma^2 = 0.8$) is used for the Gaussian likelihood (see Eq.
 420 3); for informal likelihoods (see Eq. 6) $T = 1$ is used. The likelihood thresholds are es-

421 timated to correspond to the best 2% of all simulations. For MLDA, the sub-sampling
 422 rate is set to 5. All methods are run on 50 CPUs.

423 3 Results and Discussion

424 For the two examples considered, we now present results of inversion with the method-
 425 ologies of MLGLUE, GLUE, MLDA, and MCMC. We analyze how models on different
 426 levels are related (i.e., for MLGLUE and MLDA) and how the results obtained with a
 427 multilevel approach differ from the conventional approach using a single model. Differ-
 428 ences between the different methods are discussed regarding obtained posterior distri-
 429 butions, uncertainty estimates for model output, and computational efficiency. Results
 430 of convergence analysis are given in the supporting information.

431 The resulting uncertainty estimates, parameter posterior distributions, and con-
 432 vergence behaviour are virtually identical when using either formal or informal likelihood
 433 functions in GLUE and MLGLUE. Therefore, the corresponding results are discussed
 434 with a focus on using an informal likelihood function in this section. Results from GLUE
 435 and MLGLUE using a formal likelihood are mainly given in the supporting information
 436 for both example problems.

437 MCMC chains typically exhibit a transition period where the samples approach the
 438 posterior distribution. The samples of this transition period are discarded as *burn-in* (Gallagher
 439 et al., 2009; Brunetti et al., 2023). GLUE and MLGLUE both result in independent pos-
 440 terior samples, while MCMC and MLDA result in correlated posterior samples. To com-
 441 pare both groups (GLUE & MLGLUE and MCMC & MLDA) on an equal basis, inde-
 442 pendent samples are obtained from MCMC and MLDA samples via *thinning*; only ev-
 443 ery \mathcal{K} -th sample is considered for subsequent analysis. We apply thinning such that the
 444 thinned number of samples is approximately equal to the estimated effective sample size
 445 of unthinned samples.

446 3.1 Linear Regression

447 This example considers the problem of estimating the parameters of slope and in-
 448 tercept from noisy observations of a one-dimensional linear regression model. Subsets
 449 of different size of the observed data are used on the different model levels instead of uti-
 450 lizing models with different spatial or temporal discretization. After analyzing the re-
 451 lation between the models on different levels, we assess the quality of inferences made
 452 with MLGLUE compared to other methods.

453 The relations between the three levels are shown in Fig. 5, from which it is appar-
 454 ent that $\mathbb{V}[\mathcal{F}_\ell]$ and $\mathbb{E}[\mathcal{F}_\ell]$ are approximately constant and that that $\mathbb{V}[\mathcal{F}_\ell - \mathcal{F}_{\ell-1}]$ and
 455 $\mathbb{E}[\mathcal{F}_\ell - \mathcal{F}_{\ell-1}]$ decay across all levels. Therefore, the approximation error of the likeli-
 456 hood apparently decreases in the informal case as $\ell \rightarrow L$, although this effect is su-
 457 perimposed by the influence of different numbers of observations on the likelihood.

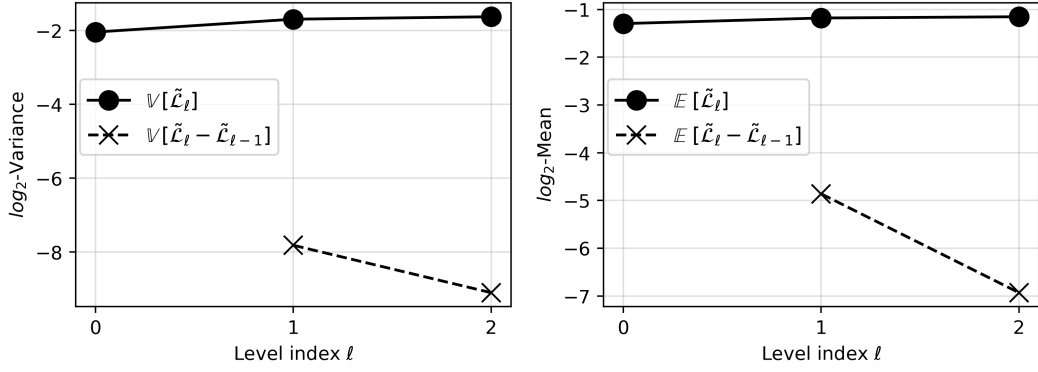


Figure 5. Relations between levels for the linear regression example, using an informal likelihood

458 The sampling efficiencies of all methods are shown in Tab. 1, showing that the number
 459 of effective samples is comparable for all methods of inference. The MLDA and MCMC
 460 computation time exceeds that of MLGLUE and GLUE by a factor ≥ 4 . GLUE is as-
 461 sociated with the highest number of effective samples per minute, followed by MLGLUE,
 462 MCMC, and MLDA. Taking the low computational cost of a single model run into ac-
 463 count, the differences in computation time can be attributed to different computational
 464 complexities of the algorithms. We also note that the initialization time of the paralleliza-
 465 tion framework dominates the overall computation times; without parallelization, the
 466 computation time is approximately one order of magnitude smaller. This effect, how-
 467 ever, diminishes when the computational cost of a single model call increases.

Table 1. Sampling efficiency for the linear regression example

Method	Time	No. of calls on $l = 2$	No. of Posterior Samples	No. of Effective Post. Sam- ples	Effective Samples per Minute
MLGLUE (I) ^a	23 s	582	300	300	782.6
MLGLUE (F) ^b	25 s	582	300	300	720.0
GLUE (I) ^a	23 s	100,000	344	344	897.4
GLUE (F) ^b	22 s	100,000	344	344	938.2
MLDA	109 s	4,000	4,000	289	159.1
MCMC	100 s	100,000	100,000	385	231.0

^aInformal likelihood

^bFormal likelihood

468 For each of the two parameters, MLGLUE and GLUE converge similarly quickly,
 469 followed by MLDA and MCMC. More detailed results of convergence analysis are shown
 470 in the supporting information.

471 Kernel density estimates of the parameter posteriors are shown in Fig. 6 (a) and
 472 (b). Posteriors for MLGLUE and GLUE are more heavy-tailed and have a smaller span,
 473 or variance, compared to the MLDA and MCMC posteriors. The distribution median
 474 is closest to the true values for both parameters for MLGLUE, followed by GLUE, MCMC,
 475 and MLDA. The more heavy-tailed posteriors of MLGLUE and GLUE may be attributed
 476 to the equifinality concept inherent to the GLUE methodology (Beven, 1993; Vrugt et
 477 al., 2009) and to the pre-defined threshold, which effectively controls the number of (ef-
 478 fective) samples as well as the distribution variance. Small deviations in slope and in-
 479 tercept parameters would still result in a high likelihood, which would be considered be-
 480 havioural with the GLUE methodology. We note that MLGLUE posterior samples are
 481 equal regardless of using a formal or an informal likelihood function. All posterior sam-
 482 ples from MLGLUE are furthermore reflected in GLUE posterior samples, which are also
 483 equal using either a formal or an informal likelihood function. 44 GLUE posterior sam-
 484 ples are not in the MLGLUE posterior samples, which can be attributed to the samples
 485 being discarded on lower levels in MLGLUE. Those sample differences are reflected in
 486 the different span and tails of the distributions.

487 Uncertainty estimates obtained from simulated values corresponding to posterior
 488 parameter samples are shown in Fig. 6. The estimates are generally similar for all meth-
 489 ods of inference, however GLUE as well as MLDA and MCMC median estimates are ini-
 490 tially more biased towards higher values than MLGLUE estimates. Coefficients of de-
 491 termination computed for median simulation and true values are virtually equal for all
 492 methods of inference. This result is in agreement with the findings of (Vrugt et al., 2009),
 493 where different posteriors from formal Bayesian inversion with MCMC and informal re-
 494 sults from GLUE would still result in similar uncertainty estimates of simulated values.

495 3.2 Groundwater Flow

496 This example considers the estimation of pilot point hydraulic conductivity values
 497 along with the length scale parameter of a Gaussian process. Four models with decreas-
 498 ing spatial resolution are considered during multilevel inversion. We analyze the rela-
 499 tions between the models on different levels, assess the quality of inferences made with
 500 MLGLUE compared to other methods of inference, and quantify computational efficiency.

501 The relations between the three levels are shown in Figs. 7, from which it is ap-
 502 parent that $\mathbb{V}[\mathcal{F}_\ell]$ and $\mathbb{E}[\mathcal{F}_\ell]$ are approximately constant and that that $\mathbb{V}[\mathcal{F}_\ell - \mathcal{F}_{\ell-1}]$ and
 503 $\mathbb{E}[\mathcal{F}_\ell - \mathcal{F}_{\ell-1}]$ decay across all levels when using the likelihood function Eq. 6. The vari-
 504 ance of the sampled likelihoods on level $\ell = 0$, however, is smaller than on higher lev-
 505 els.

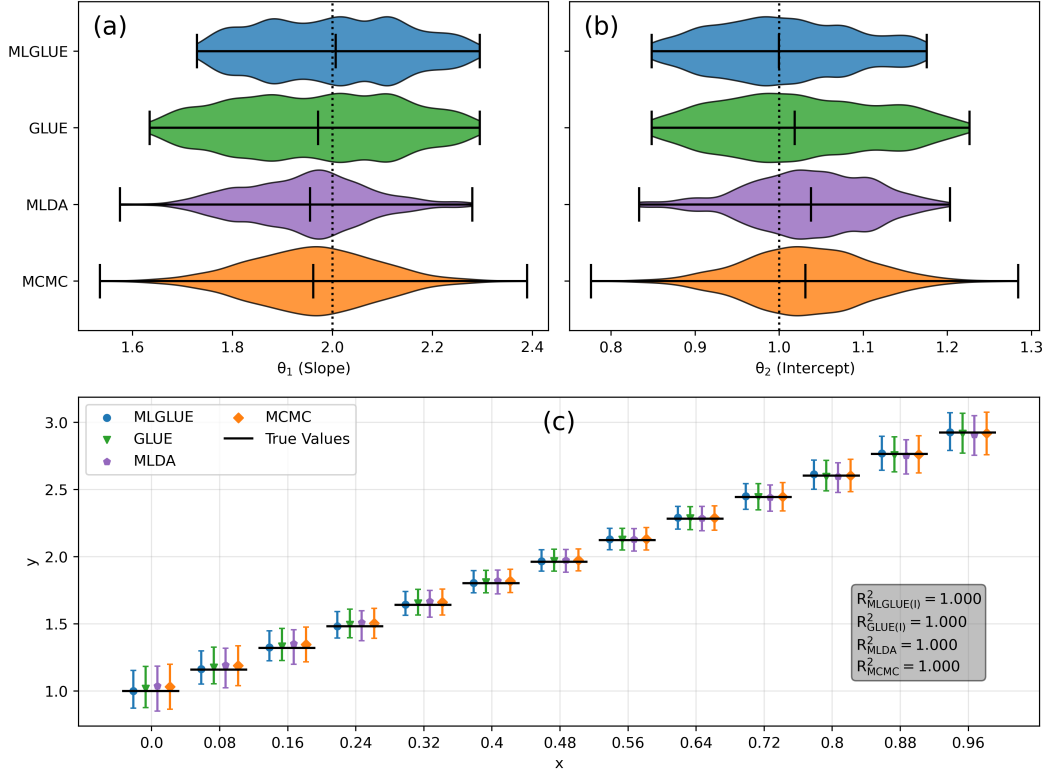


Figure 6. Kernel density estimates of model parameters, where solid vertical lines represent distribution median values and dashed lines represent the true parameter values (a, b) and 99% – 1% uncertainty estimates around the median value (c)

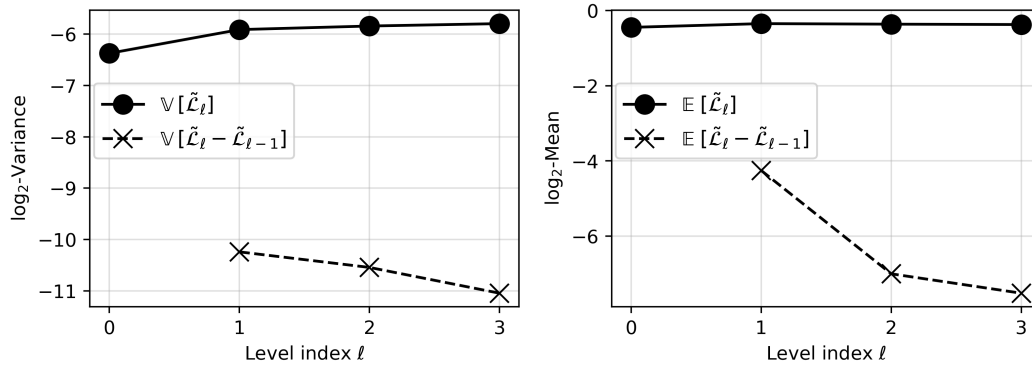


Figure 7. Relations between levels for the groundwater flow example, using an informal definition of the likelihood

506 The sampling efficiencies of all methods are shown in Tab. 2, showing that the num-
 507 ber of effective samples is comparable for all methods of inference. The computation times
 508 of single-level inference (i.e., GLUE with informal and formal likelihood and MCMC)
 509 and of multilevel inference (i.e., MLGLUE with informal and formal likelihood and MLDA)

510 are similar, respectively; the computation time of single-level inference exceeds that of
 511 multilevel inference by a factor of ≈ 2 . MLGLUE is associated with the highest num-
 512 ber of effective samples per minute, followed by GLUE, MLDA, and MCMC. This ex-
 513 ample clearly shows the benefit of using multilevel methods for inference, as overall com-
 514 putation times can be substantially reduced compared to single-level methods.

Table 2. Sampling efficiency for the groundwater flow example

Method	Time	No. of calls on $\ell = 3$	No. of Posterior Samples	No. of Effective Post. Sam- ples	Effective Samples per Minute
MLGLUE (I) ^a	1,992 <i>s</i>	1,915	331	331	10.0
MLGLUE (F) ^b	1,906 <i>s</i>	1,917	333	333	10.5
GLUE (I) ^a	3,670 <i>s</i>	100,000	398	398	6.5
GLUE (F) ^b	3,415 <i>s</i>	100,000	398	398	7.0
MLDA	2,052 <i>s</i>	800	800	267	7.8
MCMC	4,671 <i>s</i>	100,000	100,000	385	4.9

^aInformal likelihood

^bFormal likelihood

515 Averaged over all pilot point parameters, GLUE converges more quickly than MCMC,
 516 followed by MLGLUE and MLDA. However, MCMC samples converge more rapidly com-
 517 pared to MLGLUE, GLUE, and MLDA for the length scale parameter. More detailed
 518 results of convergence analysis are shown in the supporting information.

519 Kernel density estimates of the parameter posteriors are shown in Fig. 8 (a) - (d).
 520 Often, as for PP No. 3 or PP No. 38, MLGLUE and GLUE posteriors are substantially
 521 more heavy-tailed than their MLDA and MCMC counterparts. The absolute deviation
 522 of estimated posterior median values from true parameter values, averaged over all 50
 523 PP parameters, is 3.43, 3.42, 3.38, and 3.30 for MLGLUE, GLUE, MLDA, and MCMC,
 524 respectively. The equifinality concept in the GLUE methodology (Beven, 1993; Vrugt
 525 et al., 2009) manifests itself in the corresponding posterior distributions to be more heavy-
 526 tailed. The variance of the posterior distributions is furthermore controlled by the pre-
 527 defined likelihood threshold. Deviations in PP hydraulic conductivity values - in com-
 528 bination with a different GPR length scale - would still result in similar hydraulic con-
 529 ductivity fields, which is directly reflected in the more heavy-tailed MLGLUE and GLUE
 530 posteriors. PP parameters near observations points, however, are substantially more in-
 531 formed by the data, decreasing the distribution variance in MLGLUE and GLUE (see
 532 Fig. 8 (b)). MLGLUE posterior samples are highly similar regardless of using formal or
 533 informal likelihood functions, where only two additional samples are considered behavioural
 534 when using a formal likelihood function. All posterior samples from MLGLUE are fur-

535 furthermore reflected in GLUE posterior samples, which are exactly equal with a formal
 536 or informal likelihood function. Several GLUE posterior samples are not in the MLGLUE
 537 posterior samples, which can be attributed to the samples being discarded on lower lev-
 538 els with MLGLUE. Those sample differences are reflected in the different span and tails
 539 of the posteriors, which are, however, very similar.

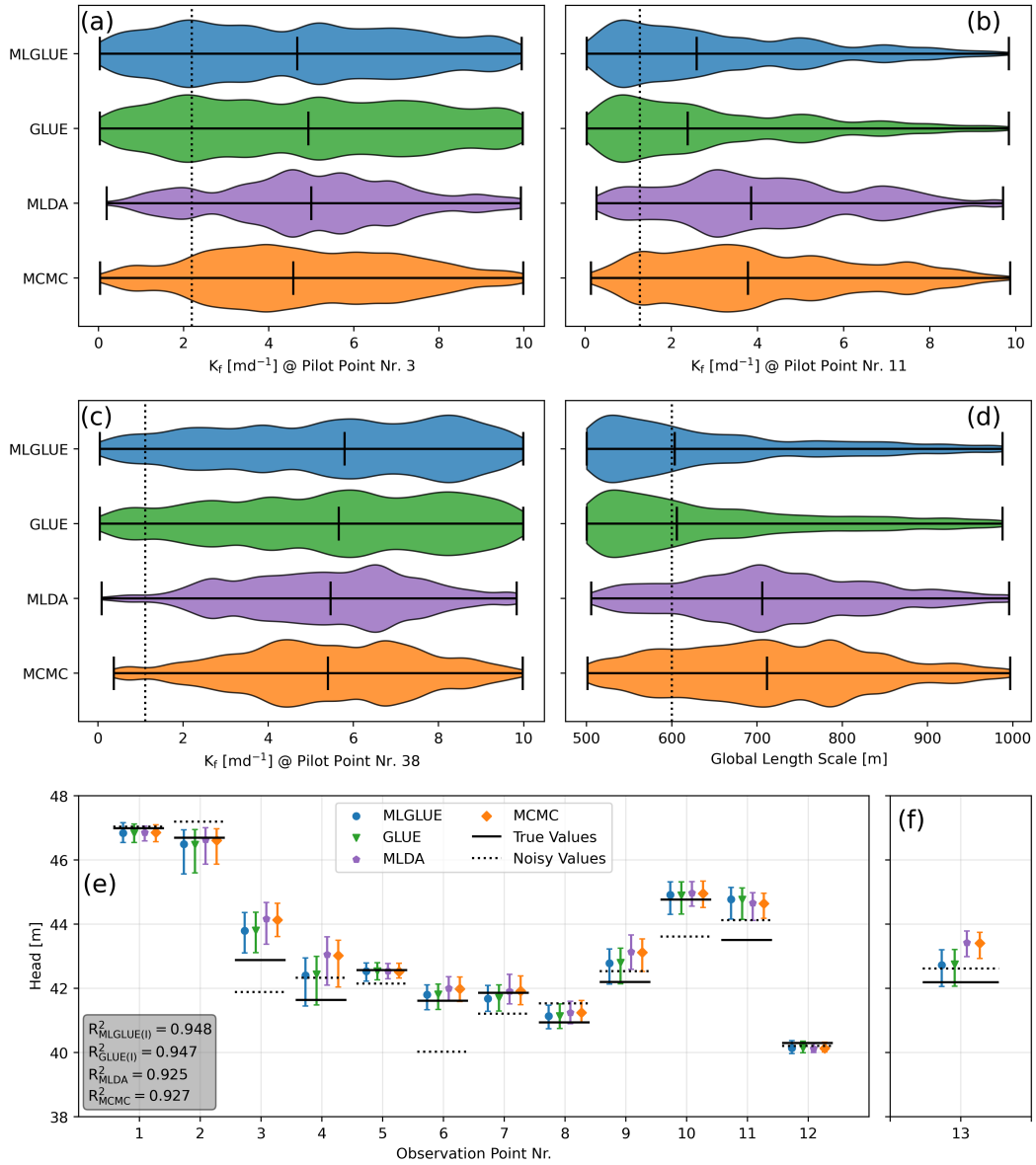


Figure 8. Kernel density estimates of model parameters, where solid vertical lines represent distribution median values and dashed lines represent the true parameter values (a, b, c, d) and 99% - 1% uncertainty estimates around the median value for observation points (e) and for the prediction point(f)

540 Uncertainty estimates obtained from simulated values corresponding to posterior
541 parameter samples are shown in Fig. 8. For observation points 1, 2, 5, 8, 10, 11, and 12,
542 the uncertainty estimates and median values are generally similar for all methods of in-
543 ference. For all other observation points as well as for the prediction point, uncertainty
544 estimates and median values from MLGLUE and GLUE reflect the true values better
545 than the MLDA and MCMC counterparts. This is also reflected in the coefficients of de-
546 termination computed for median simulation and true values. They are virtually equal
547 for MLGLUE and GLUE methods and lower values were observed for MLDA and MCMC.
548 This result is in partial agreement to the findings of (Vrugt et al., 2009), where differ-
549 ent posteriors from formal Bayesian inversion with MCMC and informal results from GLUE
550 still resulted in similar uncertainty estimates of simulated values. For multiple observa-
551 tion points, however, MLDA and MCMC estimates more strongly deviate from MLGLUE
552 and GLUE results. This can not only be attributed to the likelihood function used (as
553 the same likelihood function is used in the cases of formal MLGLUE and GLUE as well
554 as MLDA and MCMC) but also to the general approaches of a Monte Carlo type (ML-
555 GLUE and GLUE) and Markov-chain Monte-Carlo type (MLDA and MCMC); MCMC-
556 type inferences are often over-confident, especially when using uninformative prior dis-
557 tributions (Gelman et al., 2021).

558 4 Conclusions

559 In hydrological sciences, the popularity of statistical inference and inversion has
560 remained high in recent years. However, the applicability of corresponding approaches
561 to more complex models and in the context of digital twins has been limited by the as-
562 sociated computational cost when solving inverse problems. The goal of our study is to
563 introduce and test an extension to the GLUE methodology for Bayesian inversion that
564 alleviates the problems associated with computationally costly models. Concepts from
565 multilevel Monte Carlo and multilevel Markov-chain Monte Carlo methods are incorpo-
566 rated in the Generalized Likelihood Uncertainty Estimation (GLUE) methodology, re-
567 sulting in the novel multilevel GLUE (MLGLUE) algorithm. In MLGLUE, a hierarchy
568 of models with multiple resolutions (e.g., cell- or time-step sizes) are considered instead
569 of using a (data-driven) surrogate model that is decoupled from the high-fidelity or tar-
570 get model. While surrogate models have been frequently used in place of computationally
571 costly models to reduce the computational cost of statistical inversion, in MLGLUE
572 the models on different levels in the hierarchy are synergetically used together and in-
573 ferences using MLGLUE are made with respect to the target model instead of a surro-
574 gate. The evaluation of a parameter sample is initiated on the lowest level $\ell = 0$, which
575 is associated with a computationally cheap low-resolution model. The sample is only passed
576 to the next higher level $\ell + 1$, which is associated with a model of higher resolution, if
577 it results in a likelihood that is above a user defined threshold. Parameter samples are
578 only finally accepted if they reach the highest level $\ell = L$, which is associated with the
579 highest-resolution target model. Most parameter samples are evaluated (and discarded)

580 on lower levels and samples that reach the highest level are accepted with high proba-
 581 bility, which results in substantial computational savings.

582 MLGLUE is evaluated using two test cases. The results of statistical inversion with
 583 MLGLUE are compared to the results from GLUE, Markov-chain Monte Carlo (MCMC)
 584 using a sampler from the DREAM family, as well as multilevel delayed acceptance (MLDA)
 585 MCMC in combination with a base-sampler from the DREAM family. There, identical
 586 numbers of prior samples are considered for all methods to ensure comparability. We show
 587 that the results (parameter posteriors, uncertainty estimates, convergence behaviour) for
 588 MLGLUE and GLUE are highly similar or even identical for both test cases. While the
 589 identified parameter posteriors are different for both test problems between GLUE, ML-
 590 GLUE, MCMC, and MLDA, the resulting uncertainty estimates are similar. For the com-
 591 putationally more costly example of groundwater flow, MLGLUE results in the largest
 592 number of effective samples per minute and has the smallest overall computation time,
 593 reducing the time for inversion by $\approx 45\%$ and $\approx 57\%$ compared to conventional for-
 594 mulations of GLUE and MCMC, respectively. We expect the computational benefit of
 595 using MLGLUE to increase as the computational cost of a single model call increases,
 596 which has been previously identified for multilevel Monte Carlo and multilevel inversion
 597 (Cliffe et al., 2011; Giles, 2015; Dodwell et al., 2019; Lykkegaard et al., 2023).

598 As we discussed for both test cases and as mentioned by Lykkegaard et al. (2023),
 599 coarse levels should be designed carefully; i.e., lower-level models should be well corre-
 600 lated to the next higher level. While this is reflected in diagnostic plots as shown for the
 601 two examples, low or even negative correlation between levels will lead to parameter sam-
 602 ples being discarded on lower levels although they would be accepted on higher levels,
 603 resulting in a smaller number of effective samples and in a smaller acceptance probabili-
 604 ty. Besides the samples of parameters and model outputs on the highest level, MLGLUE
 605 can optionally return these and other data for each model run on any level. This data
 606 enables the (statistical) analysis of various aspects such as the impact of model resolu-
 607 tion on various quantities of interest or the possibility for model simplification. Savage
 608 et al. (2016) analyze the importance of model resolution via sensitivity analysis; analyz-
 609 ing the worth of aforementioned data from MLGLUE is an opportunity for future re-
 610 search, both in the context of multilevel methods and general model development.

611 Our results demonstrate that:

- 612 • By considering a hierarchy of models with decreasing (spatial) resolution, MLGLUE
 613 can substantially reduce the computational cost of statistical inversion for com-
 614 plex spatially distributed (groundwater) hydrological models.
- 615 • MLGLUE is most effective for PDE-based models, such as they are often encoun-
 616 tered in the hydrological sciences; notions of grid or time-step refinement and coars-
 617 ening are well understood in such cases and MLGLUE may be directly applied.
- 618 • MLGLUE can also be applied to problems with a generalized notion of resolution,
 619 e.g., when using different subsets of observation data.

MLGLUE enables statistical Bayesian inversion for models where it would previously have been computationally intractable, paving the way for more robust simulations and predictions of complex environmental systems under uncertainty.

Open Research Section

Relevant resources needed to reproduce the results as well as figures are openly available and can be found under the DOI [10.5281/zenodo.10018088](https://doi.org/10.5281/zenodo.10018088) (Rudolph et al., 2023). The MLGLUE algorithm is available as a Python package under <https://github.com/iGW-TU-Dresden/MLGLUE>.

Acknowledgments

Funding for Thorsten Wagener has been provided by the Alexander von Humboldt Foundation in the framework of the Alexander von Humboldt Professorship endowed by the German Federal Ministry of Education and Research. The authors thank Robert Scheichl, Aretha Teckentrup, and Anastasia Istratuca for fruitful discussions and inspiration. The authors have no conflict of interest with respect to the results of this study.

References

- Allgeier, J. T. (2022). *Analytical and Stochastic Numerical Methods for the Simulation of Subsurface Flow in Floodplains* (Unpublished doctoral dissertation). Eberhard Karls Universität Tübingen, Tübingen.
- Anderson, M. P., Woessner, W. W., & Hunt, R. J. (2015). *Applied groundwater modeling: simulation of flow and advective transport* (Second edition ed.). London ; San Diego, CA: Academic Press. (OCLC: ocn921253555)
- Asher, M. J., Croke, B. F. W., Jakeman, A. J., & Peeters, L. J. M. (2015, August). A review of surrogate models and their application to groundwater modeling: SURROGATES OF GROUNDWATER MODELS. *Water Resources Research*, *51*(8), 5957–5973. Retrieved 2022-07-13, from <http://doi.wiley.com/10.1002/2015WR016967> doi: 10.1002/2015WR016967
- Beven, K. (1993). Prophecy, reality and uncertainty in distributed hydrological modelling. *Advances in Water Resources*, *16*(1), 41–51. Retrieved 2023-05-23, from <https://linkinghub.elsevier.com/retrieve/pii/030917089390028E> doi: 10.1016/0309-1708(93)90028-E
- Beven, K. (2006, March). A manifesto for the equifinality thesis. *Journal of Hydrology*, *320*(1-2), 18–36. Retrieved 2022-02-25, from <https://linkinghub.elsevier.com/retrieve/pii/S002216940500332X> doi: 10.1016/j.jhydrol.2005.07.007
- Beven, K. (2016, July). Facets of uncertainty: epistemic uncertainty, non-stationarity, likelihood, hypothesis testing, and communication. *Hydrological Sciences Journal*, *61*(9), 1652–1665. Retrieved 2023-10-04, from <http://www.tandfonline.com/doi/full/10.1080/02626667.2015.1031761>

- doi: 10.1080/02626667.2015.1031761
- 658 Beven, K., & Binley, A. (1992, July). The future of distributed models: Model
659 calibration and uncertainty prediction. *Hydrological Processes*, 6(3), 279–
660 298. Retrieved 2022-05-25, from [https://onlinelibrary.wiley.com/doi/](https://onlinelibrary.wiley.com/doi/10.1002/hyp.3360060305)
661 [10.1002/hyp.3360060305](https://onlinelibrary.wiley.com/doi/10.1002/hyp.3360060305) doi: 10.1002/hyp.3360060305
- 662 Beven, K., & Binley, A. (2014, November). GLUE: 20 years on. *Hy-*
663 *drological Processes*, 28(24), 5897–5918. Retrieved 2023-01-09, from
664 <https://onlinelibrary.wiley.com/doi/10.1002/hyp.10082> doi:
665 10.1002/hyp.10082
- 666 Beven, K., & Freer, J. (2001). Equifinality, data assimilation, and uncertainty esti-
667 mation in mechanistic modelling of complex environmental systems using the
668 GLUE methodology. *Journal of Hydrology*, 19.
- 669 Binley, A., Beven, K., & Elgy, J. (1989, June). A physically based model of hetero-
670 geneous hillslopes: 2. Effective hydraulic conductivities. *Water Resources Re-*
671 *search*, 25(6), 1227–1233. Retrieved 2023-05-26, from [http://doi.wiley.com/](http://doi.wiley.com/10.1029/WR025i006p01227)
672 [10.1029/WR025i006p01227](http://doi.wiley.com/10.1029/WR025i006p01227) doi: 10.1029/WR025i006p01227
- 673 Blöschl, G., Bierkens, M. F., Chambel, A., Cudennec, C., Destouni, G., Fiori, A., ...
674 Zhang, Y. (2019, July). Twenty-three unsolved problems in hydrology (UPH)
675 – a community perspective. *Hydrological Sciences Journal*, 64(10), 1141–
676 1158. Retrieved 2023-10-04, from [https://www.tandfonline.com/doi/full/](https://www.tandfonline.com/doi/full/10.1080/02626667.2019.1620507)
677 [10.1080/02626667.2019.1620507](https://www.tandfonline.com/doi/full/10.1080/02626667.2019.1620507) doi: 10.1080/02626667.2019.1620507
- 678 Brunetti, G., Šimunek, J., Wöhling, T., & Stumpp, C. (2023, September). An
679 in-depth analysis of Markov-Chain Monte Carlo ensemble samplers for in-
680 verse vadose zone modeling. *Journal of Hydrology*, 624, 129822. Retrieved
681 2023-10-04, from [https://linkinghub.elsevier.com/retrieve/pii/](https://linkinghub.elsevier.com/retrieve/pii/S0022169423007643)
682 [S0022169423007643](https://linkinghub.elsevier.com/retrieve/pii/S0022169423007643) doi: 10.1016/j.jhydrol.2023.129822
- 683 Burrows, W., & Doherty, J. E. (2015, July). Efficient Calibration/Uncertainty
684 Analysis Using Paired Complex/Surrogate Models. *Groundwater*, 53(4), 531–
685 541. Retrieved 2022-05-16, from [https://onlinelibrary.wiley.com/doi/](https://onlinelibrary.wiley.com/doi/10.1111/gwat.12257)
686 [10.1111/gwat.12257](https://onlinelibrary.wiley.com/doi/10.1111/gwat.12257) doi: 10.1111/gwat.12257
- 687 Carrera, J., Alcolea, A., Medina, A., Hidalgo, J., & Slooten, L. J. (2005, March).
688 Inverse problem in hydrogeology. *Hydrogeology Journal*, 13(1), 206–
689 222. Retrieved 2023-05-22, from [http://link.springer.com/10.1007/](http://link.springer.com/10.1007/s10040-004-0404-7)
690 [s10040-004-0404-7](http://link.springer.com/10.1007/s10040-004-0404-7) doi: 10.1007/s10040-004-0404-7
- 691 Christen, J. A., & Fox, C. (2005). Markov Chain Monte Carlo Using an Approxima-
692 tion. *Journal of Computational and Graphical Statistics*, 14(4). doi: 10.1198/
693 106186005X76983
- 694 Cliffe, K. A., Giles, M. B., Scheichl, R., & Teckentrup, A. L. (2011, January). Mul-
695 tilevel Monte Carlo methods and applications to elliptic PDEs with random
696 coefficients. *Computing and Visualization in Science*, 14(1), 3–15. Retrieved
697 2022-11-23, from <http://link.springer.com/10.1007/s00791-011-0160-x>
698 doi: 10.1007/s00791-011-0160-x
- 699 Colecchio, I., Boschan, A., Otero, A. D., & Noetinger, B. (2020, June). On
700

- 701 the multiscale characterization of effective hydraulic conductivity in ran-
 702 dom heterogeneous media: A historical survey and some new perspectives.
 703 *Advances in Water Resources*, 140, 103594. Retrieved 2023-05-26, from
 704 <https://linkinghub.elsevier.com/retrieve/pii/S0309170819310681>
 705 doi: 10.1016/j.advwatres.2020.103594
- 706 Dodwell, T. J., Ketelsen, C., Scheichl, R., & Teckentrup, A. L. (2019). Multilevel
 707 Markov Chain Monte Carlo. *SIAM / ASA Journal of Uncertainty Quantifica-*
 708 *tion*.
- 709 Doherty, J. E. (2003, March). Ground Water Model Calibration Using Pilot Points
 710 and Regularization. *Groundwater*, 41(2), 170–177. Retrieved 2022-07-11, from
 711 <https://doi.org/10.1111/j.1745-6584.2003.tb02580.x> (Publisher: John
 712 Wiley & Sons, Ltd) doi: 10.1111/j.1745-6584.2003.tb02580.x
- 713 Doherty, J. E. (2015). *Calibration and Uncertainty Analysis for Complex Environ-*
 714 *mental Models*. Brisbane: Watermark Numerical Computing.
- 715 Doherty, J. E., & Christensen, S. (2011, December). Use of paired simple and
 716 complex models to reduce predictive bias and quantify uncertainty. *Water Re-*
 717 *sources Research*, 47(12). Retrieved 2022-02-28, from [http://doi.wiley.com/](http://doi.wiley.com/10.1029/2011WR010763)
 718 [10.1029/2011WR010763](http://doi.wiley.com/10.1029/2011WR010763) doi: 10.1029/2011WR010763
- 719 Erdal, D., & Cirpka, O. A. (2020, September). Technical Note: Improved sampling
 720 of behavioral subsurface flow model parameters using active subspaces. *Hydrol-*
 721 *ogy and Earth System Sciences*, 24(9), 4567–4574. Retrieved 2023-10-04, from
 722 <https://hess.copernicus.org/articles/24/4567/2020/> doi: 10.5194/hess-
 723 -24-4567-2020
- 724 Gallagher, K., Charvin, K., Nielsen, S., Sambridge, M., & Stephenson, J. (2009,
 725 April). Markov chain Monte Carlo (MCMC) sampling methods to deter-
 726 mine optimal models, model resolution and model choice for Earth Science
 727 problems. *Marine and Petroleum Geology*, 26(4), 525–535. Retrieved
 728 2023-10-04, from [https://linkinghub.elsevier.com/retrieve/pii/](https://linkinghub.elsevier.com/retrieve/pii/S0264817209000075)
 729 [S0264817209000075](https://linkinghub.elsevier.com/retrieve/pii/S0264817209000075) doi: 10.1016/j.marpetgeo.2009.01.003
- 730 Gelman, A., Carlin, J. B., Stern, H. S., Dunson, D. B., Vehtari, A., & Rubin, D. B.
 731 (2021). *Bayesian Data Analysis* (3rd ed.).
- 732 Gelman, A., & Rubin, D. B. (1992, November). Inference from Iterative Simulation
 733 Using Multiple Sequences. *Statistical Science*, 7(4). Retrieved 2022-11-08, from
 734 [https://projecteuclid.org/journals/statistical-science/volume-7/](https://projecteuclid.org/journals/statistical-science/volume-7/issue-4/Inference-from-Iterative-Simulation-Using-Multiple-Sequences/10.1214/ss/1177011136.full)
 735 [issue-4/Inference-from-Iterative-Simulation-Using-Multiple](https://projecteuclid.org/journals/statistical-science/volume-7/issue-4/Inference-from-Iterative-Simulation-Using-Multiple-Sequences/10.1214/ss/1177011136.full)
 736 [-Sequences/10.1214/ss/1177011136.full](https://projecteuclid.org/journals/statistical-science/volume-7/issue-4/Inference-from-Iterative-Simulation-Using-Multiple-Sequences/10.1214/ss/1177011136.full) doi: 10.1214/ss/1177011136
- 737 Giles, M. B. (2008, June). Multilevel Monte Carlo Path Simulation. *Opera-*
 738 *tions Research*, 56(3), 607–617. Retrieved 2023-05-02, from [https://doi.org/](https://doi.org/10.1287/opre.1070.0496)
 739 [10.1287/opre.1070.0496](https://doi.org/10.1287/opre.1070.0496) (Publisher: INFORMS) doi: 10.1287/opre.1070
 740 .0496
- 741 Giles, M. B. (2015, May). Multilevel Monte Carlo methods. *Acta Numerica*,
 742 24, 259–328. Retrieved 2022-11-24, from [https://www.cambridge.org/core/](https://www.cambridge.org/core/product/identifier/S096249291500001X/type/journal_article)
 743 [product/identifier/S096249291500001X/type/journal_article](https://www.cambridge.org/core/product/identifier/S096249291500001X/type/journal_article) doi: 10

- 744 .1017/S096249291500001X
- 745 Gosses, M., & Wöhling, T. (2019, March). Simplification error analysis for ground-
 746 water predictions with reduced order models. *Advances in Water Resources*,
 747 *125*, 41–56. Retrieved 2022-02-17, from [https://linkinghub.elsevier.com/
 748 retrieve/pii/S030917081830575X](https://linkinghub.elsevier.com/retrieve/pii/S030917081830575X) doi: 10.1016/j.advwatres.2019.01.006
- 749 Gosses, M., & Wöhling, T. (2021, September). Robust Data Worth Analysis with
 750 Surrogate Models. *Groundwater*, *59*(5), 728–744. Retrieved 2022-05-12,
 751 from <https://onlinelibrary.wiley.com/doi/10.1111/gwat.13098> doi:
 752 10.1111/gwat.13098
- 753 Harbaugh, A. W. (2005). *MODFLOW-2005, The U.S. Geological Survey Modular*
 754 *Ground-Water Model—the Ground-Water Flow Process* (Tech. Rep. No. U.S.
 755 Geological Survey Techniques and Methods 6–A16). Reston, VA: USGS.
- 756 Heinrich, S. (2001). Multilevel Monte Carlo Methods. In S. Margenov,
 757 J. Waśniewski, & P. Yalamov (Eds.), *Large-Scale Scientific Computing* (pp.
 758 58–67). Berlin, Heidelberg: Springer Berlin Heidelberg.
- 759 Herrera, P. A., Marazuela, M. A., & Hofmann, T. (2022, January). Parameter
 760 estimation and uncertainty analysis in hydrological modeling. *WIREs Wa-*
 761 *ter*, *9*(1), e1569. Retrieved 2023-10-04, from [https://wires.onlinelibrary
 762 .wiley.com/doi/10.1002/wat2.1569](https://wires.onlinelibrary.wiley.com/doi/10.1002/wat2.1569) doi: 10.1002/wat2.1569
- 763 Kavetski, D., Kuczera, G., & Franks, S. W. (2006, March). Bayesian analysis
 764 of input uncertainty in hydrological modeling: 1. Theory: INPUT UNCER-
 765 TAINTY IN HYDROLOGY, 1. *Water Resources Research*, *42*(3). Retrieved
 766 2022-11-30, from <http://doi.wiley.com/10.1029/2005WR004368> doi:
 767 10.1029/2005WR004368
- 768 Kitanidis, P. K., & Vomvoris, E. G. (1983, June). A geostatistical approach to the
 769 inverse problem in groundwater modeling (steady state) and one-dimensional
 770 simulations. *Water Resources Research*, *19*(3), 677–690. Retrieved 2023-
 771 05-25, from <http://doi.wiley.com/10.1029/WR019i003p00677> doi:
 772 10.1029/WR019i003p00677
- 773 Kuffour, B. N. O., Engdahl, N. B., Woodward, C. S., Condon, L. E., Kollet, S.,
 774 & Maxwell, R. M. (2020, March). Simulating coupled surface–subsurface
 775 flows with ParFlow v3.5.0: capabilities, applications, and ongoing develop-
 776 ment of an open-source, massively parallel, integrated hydrologic model.
 777 *Geoscientific Model Development*, *13*(3), 1373–1397. Retrieved 2023-10-
 778 04, from <https://gmd.copernicus.org/articles/13/1373/2020/> doi:
 779 10.5194/gmd-13-1373-2020
- 780 Kumar, R., Carroll, C., Hartikainen, A., & Martin, O. (2019). ArviZ a unified li-
 781 brary for exploratory analysis of Bayesian models in Python. *Journal of Open*
 782 *Source Software*, *4*(33), 1143. Retrieved from [https://doi.org/10.21105/
 783 joss.01143](https://doi.org/10.21105/joss.01143) (Publisher: The Open Journal) doi: 10.21105/joss.01143
- 784 Kumar, R., Samaniego, L., & Attinger, S. (2013, January). Implications of dis-
 785 tributed hydrologic model parameterization on water fluxes at multiple
 786 scales and locations: DISTRIBUTED HYDROLOGIC MODEL PARAM-

- 787 ETERIZATIONS. *Water Resources Research*, 49(1), 360–379. Retrieved
 788 2023-05-23, from <http://doi.wiley.com/10.1029/2012WR012195> doi:
 789 10.1029/2012WR012195
- 790 Leopoldina, G. N. A. o. S. (Ed.). (2022). *Earth system science: Dis-*
 791 *covery, diagnosis, and solutions in times of global change : Re-*
 792 *port on tomorrow's science.* Retrieved from [https://levana](https://levana.leopoldina.org/receive/leopoldina_mods_00591)
 793 [.leopoldina.org/receive/leopoldina_mods_00591](https://levana.leopoldina.org/receive/leopoldina_mods_00591) (ISBN: 978-
 794 3-8047-4256-7 Url: https://doi.org/10.26164/leopoldina_03-00590 Url:
 795 https://doi.org/10.26164/leopoldina_03-00591) doi: 10.26164/leopoldina_03
 796 _00591
- 797 Linde, N., Ginsbourger, D., Irving, J., Nobile, F., & Doucet, A. (2017, Decem-
 798 ber). On uncertainty quantification in hydrogeology and hydrogeophysics.
 799 *Advances in Water Resources*, 110, 166–181. Retrieved 2023-05-16, from
 800 <https://linkinghub.elsevier.com/retrieve/pii/S0309170817304608>
 801 doi: 10.1016/j.advwatres.2017.10.014
- 802 Liu, J. S. (Ed.). (2008). *Monte Carlo Strategies in Scientific Computing*. New York:
 803 Springer.
- 804 Liu, Y., Li, J., Sun, S., & Yu, B. (2019, October). Advances in Gaussian ran-
 805 dom field generation: a review. *Computational Geosciences*, 23(5), 1011–
 806 1047. Retrieved 2022-08-31, from [http://link.springer.com/10.1007/](http://link.springer.com/10.1007/s10596-019-09867-y)
 807 [s10596-019-09867-y](http://link.springer.com/10.1007/s10596-019-09867-y) doi: 10.1007/s10596-019-09867-y
- 808 Lykkegaard, M. B. (2022, November). *tinyDA*. Retrieved from [https://pypi.org/](https://pypi.org/project/tinyda/)
 809 [project/tinyda/](https://pypi.org/project/tinyda/)
- 810 Lykkegaard, M. B., & Dodwell, T. J. (2022, June). Where to drill next? A
 811 dual-weighted approach to adaptive optimal design of groundwater surveys.
 812 *Advances in Water Resources*, 164, 104219. Retrieved 2023-01-16, from
 813 <https://linkinghub.elsevier.com/retrieve/pii/S0309170822000914>
 814 doi: 10.1016/j.advwatres.2022.104219
- 815 Lykkegaard, M. B., Dodwell, T. J., Fox, C., Mingas, G., & Scheichl, R. (2023,
 816 March). Multilevel Delayed Acceptance MCMC. *SIAM/ASA Journal on Un-*
 817 *certainty Quantification*, 11(1), 1–30. Retrieved 2023-03-16, from [https://](https://epubs.siam.org/doi/10.1137/22M1476770)
 818 epubs.siam.org/doi/10.1137/22M1476770 doi: 10.1137/22M1476770
- 819 Mai, J. (2023, May). Ten strategies towards successful calibration of environmen-
 820 tal models. *Journal of Hydrology*, 620, 129414. Retrieved 2023-06-01, from
 821 <https://linkinghub.elsevier.com/retrieve/pii/S0022169423003566>
 822 doi: 10.1016/j.jhydrol.2023.129414
- 823 Mirzaei, M., Huang, Y. F., El-Shafie, A., & Shatirah, A. (2015, July). Applica-
 824 tion of the generalized likelihood uncertainty estimation (GLUE) approach
 825 for assessing uncertainty in hydrological models: a review. *Stochastic En-*
 826 *vironmental Research and Risk Assessment*, 29(5), 1265–1273. Retrieved
 827 2023-05-03, from <http://link.springer.com/10.1007/s00477-014-1000-6>
 828 doi: 10.1007/s00477-014-1000-6
- 829 Montanari, A. (2007, March). What do we mean by ‘uncertainty’? The need

- 830 for a consistent wording about uncertainty assessment in hydrology. *Hy-*
 831 *drological Processes*, 21(6), 841–845. Retrieved 2022-11-30, from [https://](https://onlinelibrary.wiley.com/doi/10.1002/hyp.6623)
 832 onlinelibrary.wiley.com/doi/10.1002/hyp.6623 doi: 10.1002/hyp.6623
- 833 Moore, C., & Doherty, J. E. (2006, April). The cost of uniqueness in groundwa-
 834 ter model calibration. *Advances in Water Resources*, 29(4), 605–623. Re-
 835 trieved 2022-07-13, from [https://linkinghub.elsevier.com/retrieve/pii/](https://linkinghub.elsevier.com/retrieve/pii/S0309170805001752)
 836 [S0309170805001752](https://linkinghub.elsevier.com/retrieve/pii/S0309170805001752) doi: 10.1016/j.advwatres.2005.07.003
- 837 Moore, C., Wöhling, T., & Doherty, J. (2010, August). Efficient regularization and
 838 uncertainty analysis using a global optimization methodology: REGULAR-
 839 IZATION, UNCERTAINTY AND GLOBAL OPTIMIZATION. *Water Re-*
 840 *sources Research*, 46(8). Retrieved 2023-10-16, from [http://doi.wiley.com/](http://doi.wiley.com/10.1029/2009WR008627)
 841 [10.1029/2009WR008627](http://doi.wiley.com/10.1029/2009WR008627) doi: 10.1029/2009WR008627
- 842 Niswonger, R. G., Panday, S., & Ibaraki, M. (2011). *MODFLOW-NWT, A Newton*
 843 *formulation for MODFLOW-2005* (Tech. Rep. No. U.S. Geological Survey
 844 Techniques and Methods 6–A37).
- 845 Nott, D. J., Marshall, L., & Brown, J. (2012, December). Generalized likelihood un-
 846 certainty estimation (GLUE) and approximate Bayesian computation: What’s
 847 the connection?: TECHNICAL NOTE. *Water Resources Research*, 48(12).
 848 Retrieved 2023-05-03, from <http://doi.wiley.com/10.1029/2011WR011128>
 849 doi: 10.1029/2011WR011128
- 850 Page, T., Smith, P., Beven, K., Pianosi, F., Sarrazin, F., Almeida, S., ... Wagener,
 851 T. (2023, July). Technical note: The CREDIBLE Uncertainty Estimation
 852 (CURE) toolbox: facilitating the communication of epistemic uncertainty.
 853 *Hydrology and Earth System Sciences*, 27(13), 2523–2534. Retrieved 2023-
 854 10-04, from <https://hess.copernicus.org/articles/27/2523/2023/> doi:
 855 10.5194/hess-27-2523-2023
- 856 Pedregosa, F., Varoquaux, G., Gramfort, A., Michel, V., Thirion, B., Grisel, O., ...
 857 Duchesnay, E. (2011). Scikit-learn: Machine learning in Python. *Journal of*
 858 *Machine Learning Research*, 12, 2825–2830.
- 859 Pokhrel, P., Gupta, H. V., & Wagener, T. (2008, December). A spatial regulariza-
 860 tion approach to parameter estimation for a distributed watershed model. *Wa-*
 861 *ter Resources Research*, 44(12), 2007WR006615. Retrieved 2023-10-16, from
 862 <https://agupubs.onlinelibrary.wiley.com/doi/10.1029/2007WR006615>
 863 doi: 10.1029/2007WR006615
- 864 Rudolph, M. G., Wöhling, T., Wagener, T., & Hartmann, A. (2023, October). *Ex-*
 865 *tending GLUE with Multilevel Methods to Accelerate Statistical Inversion of*
 866 *Hydrological Models - Code and Data, [Code and Data]*. Zenodo. Retrieved
 867 from doi.org/10.5281/zenodo.10018088
- 868 Sadegh, M., & Vrugt, J. A. (2013, December). Bridging the gap between GLUE
 869 and formal statistical approaches: approximate Bayesian computation. *Hydro-*
 870 *logy and Earth System Sciences*, 117(12), 4831–4850. Retrieved 2023-05-03, from
 871 <https://hess.copernicus.org/articles/17/4831/2013/> doi: 10.5194/hess-
 872 -17-4831-2013

- 873 Samaniego, L., Kumar, R., & Attinger, S. (2010, May). Multiscale parameter region-
 874 alization of a grid-based hydrologic model at the mesoscale: MULTISCALE
 875 PARAMETER REGIONALIZATION. *Water Resources Research*, *46*(5). Re-
 876 trieved 2023-05-23, from <http://doi.wiley.com/10.1029/2008WR007327> doi:
 877 10.1029/2008WR007327
- 878 Savage, J. T. S., Pianosi, F., Bates, P., Freer, J., & Wagener, T. (2016, Novem-
 879 ber). Quantifying the importance of spatial resolution and other fac-
 880 tors through global sensitivity analysis of a flood inundation model. *Wa-
 881 ter Resources Research*, *52*(11), 9146–9163. Retrieved 2023-10-04, from
 882 <https://agupubs.onlinelibrary.wiley.com/doi/10.1002/2015WR018198>
 883 doi: 10.1002/2015WR018198
- 884 Team, R. (2022). *Ray*. Retrieved from <https://pypi.org/project/ray/2.2.0/>
- 885 Tonkin, M. J., & Doherty, J. E. (2005, October). A hybrid regularized inversion
 886 methodology for highly parameterized environmental models: HYBRID REG-
 887 ULARIZATION METHODOLOGY. *Water Resources Research*, *41*(10).
 888 Retrieved 2022-05-16, from <http://doi.wiley.com/10.1029/2005WR003995>
 889 doi: 10.1029/2005WR003995
- 890 von Gunten, D., Wöhling, T., Haslauer, C., Merchán, D., Causapé, J., & Cirpka,
 891 O. A. (2014, November). Efficient calibration of a distributed pde -based hy-
 892 drological model using grid coarsening. *Journal of Hydrology*, *519*, 3290–3304.
 893 Retrieved 2023-03-03, from [https://linkinghub.elsevier.com/retrieve/
 894 pii/S0022169414008191](https://linkinghub.elsevier.com/retrieve/pii/S0022169414008191) doi: 10.1016/j.jhydrol.2014.10.025
- 895 Vrugt, J. A. (2016, January). Markov chain Monte Carlo simulation using the
 896 DREAM software package: Theory, concepts, and MATLAB implementation.
 897 *Environmental Modelling & Software*, *75*, 273–316. Retrieved 2022-07-19, from
 898 <https://linkinghub.elsevier.com/retrieve/pii/S1364815215300396>
 899 doi: 10.1016/j.envsoft.2015.08.013
- 900 Vrugt, J. A., & Beven, K. J. (2018, April). Embracing equifinality with effi-
 901 ciency: Limits of Acceptability sampling using the DREAM(LOA) algo-
 902 rithm. *Journal of Hydrology*, *559*, 954–971. Retrieved 2023-10-04, from
 903 <https://linkinghub.elsevier.com/retrieve/pii/S0022169418301021>
 904 doi: 10.1016/j.jhydrol.2018.02.026
- 905 Vrugt, J. A., ter Braak, C. J. F., Gupta, H. V., & Robinson, B. A. (2009, Oc-
 906 tober). Equifinality of formal (DREAM) and informal (GLUE) Bayesian
 907 approaches in hydrologic modeling? *Stochastic Environmental Re-
 908 search and Risk Assessment*, *23*(7), 1011–1026. Retrieved 2022-03-07,
 909 from <http://link.springer.com/10.1007/s00477-008-0274-y> doi:
 910 10.1007/s00477-008-0274-y
- 911 White, J. T. (2018, November). A model-independent iterative ensemble smoother
 912 for efficient history-matching and uncertainty quantification in very high
 913 dimensions. *Environmental Modelling & Software*, *109*, 191–201. Re-
 914 trieved from [https://www.sciencedirect.com/science/article/pii/
 915 S1364815218302676](https://www.sciencedirect.com/science/article/pii/S1364815218302676) doi: 10.1016/j.envsoft.2018.06.009

- 916 White, J. T., Hunt, R. J., Fienen, M. N., & Doherty, J. E. (2020). *Approaches*
917 *to highly parameterized inversion: PEST++ Version 5, a software suite*
918 *for parameter estimation, uncertainty analysis, management optimization*
919 *and sensitivity analysis* (Report No. 7-C26). Reston, VA. Retrieved from
920 <http://pubs.er.usgs.gov/publication/tm7C26> doi: 10.3133/tm7C26
- 921 White, J. T., Knowling, M. J., & Moore, C. R. (2020, September). Consequences
922 of Groundwater-Model Vertical Discretization in Risk-Based Decision-
923 Making. *Groundwater*, 58(5), 695–709. Retrieved 2022-07-06, from
924 <https://doi.org/10.1111/gwat.12957> (Publisher: John Wiley & Sons,
925 Ltd) doi: 10.1111/gwat.12957
- 926 Wildemeersch, S., Goderniaux, P., Orban, P., Brouyère, S., & Dassargues, A. (2014,
927 March). Assessing the effects of spatial discretization on large-scale flow model
928 performance and prediction uncertainty. *Journal of Hydrology*, 510, 10–25.
929 Retrieved 2023-03-17, from [https://linkinghub.elsevier.com/retrieve/](https://linkinghub.elsevier.com/retrieve/pii/S0022169413009177)
930 [pii/S0022169413009177](https://linkinghub.elsevier.com/retrieve/pii/S0022169413009177) doi: 10.1016/j.jhydrol.2013.12.020
- 931 Zhou, H., Gómez-Hernández, J. J., & Li, L. (2014, January). Inverse methods in
932 hydrogeology: Evolution and recent trends. *Advances in Water Resources*,
933 63, 22–37. Retrieved 2022-04-22, from [https://linkinghub.elsevier.com/](https://linkinghub.elsevier.com/retrieve/pii/S0309170813002017)
934 [retrieve/pii/S0309170813002017](https://linkinghub.elsevier.com/retrieve/pii/S0309170813002017) doi: 10.1016/j.advwatres.2013.10.014
- 935 Zimmerman, D. A., de Marsily, G., Gotway, C. A., Marietta, M. G., Axness, C. L.,
936 Beauheim, R. L., ... Rubin, Y. (1998, June). A comparison of seven geosta-
937 tistically based inverse approaches to estimate transmissivities for modeling
938 advective transport by groundwater flow. *Water Resources Research*, 34(6),
939 1373–1413. Retrieved 2022-05-25, from [http://doi.wiley.com/10.1029/](http://doi.wiley.com/10.1029/98WR00003)
940 [98WR00003](http://doi.wiley.com/10.1029/98WR00003) doi: 10.1029/98WR00003